

Original research article

Techno-economic evaluation and resource assessment of hydrogen production through offshore wind farms: A European perspective

Antoine Rogeau ^{a,b,*}, Julien Vieubled ^b, Matthieu de Coatpont ^b, Pedro Affonso Nobrega ^a, Guillaume Erbs ^b, Robin Girard ^a

^a Mines Paris, PSL University, Centre for processes, renewable energy and energy systems (PERSEE), Sophia Antipolis, 06904, France

^b ENGIE Impact, 1 place Samuel de Champlain, Courbevoie, 92400, France



ARTICLE INFO

Dataset link: <https://doi.org/10.5281/zenodo.8036703>

Keywords:

Hydrogen
Wind power
Wind-to-hydrogen
Offshore
Resource assessment
Electrolysis
Levelized cost of energy
Geographical information system
Cost modeling

ABSTRACT

The demand for hydrogen is expected to increase radically in the coming years, as it is an important lever for decarbonization and offshore wind is a credible option for running electrolyzers. A unified and detailed cost modeling is produced from the sparse literature that considers a variety of configurations (onshore, centralized offshore, and decentralized offshore electrolysis). A resource assessment at European scale is performed by combining the developed cost modeling with a geospatial analysis considering the levelized cost of hydrogen (LCOH). Geolocated power generation as well as technical and environmental constraints are considered to improve the assessment.

The results reveal enormous resources in European seas, with LCOH falling from 4.5–7.5 €/kg in 2020 to 1.5–3.0 €/kg in 2050 as the costs of wind turbines and electrolyzers decrease. More than 1000 TWh of green hydrogen could be produced at a price of less than 3.0 €/kg in 2030 and 2.0 €/kg in 2050, making it competitive with gray hydrogen. A valuable resource of 200 TWh is identified in 2030 where offshore wind-to-hydrogen projects have a much lower LCOH than their wind-to-power counterparts. The results, provided at the country level, are valuable for energy modelers and local stakeholders. Finally, a detailed cost analysis shows that offshore electrolysis is becoming more relevant over time: In 2020, offshore electrolysis is preferred only for far-from-shore and deepwater seas while in 2030 it is closer to shore (over 100 km). In 2050, onshore electrolysis is only relevant for nearshore and shallow waters.

1. Introduction

1.1. Context

The energy transition needed to address the global environmental crisis can take several forms. While energy efficiency and sufficiency are the two most important levers for a cleaner future, the substitution of fossil fuels with cleaner alternatives plays an important role. Electrification is often cited as the most important option for decarbonization, along with reducing the carbon content of the electricity mix. Nevertheless, some applications cannot be fully and directly electrified, mainly in industry (chemistry [1,2], steel production [3–5], and heavy industry [6]), but also in heavy transport [7]. In these cases, hydrogen proves to be a credible option for decarbonization [7–9].

Consequently, hydrogen demand – estimated at 339 TWh in Europe in 2019 [10] – is expected to increase drastically by 2050 and could

reach up to 2300 TWh in 2050 according to the European Hydrogen Backbone initiative [11], or even higher quantities depending on the scenario [12]. Today, hydrogen is mainly produced by steam methane reforming [13], a process associated with high greenhouse gas emissions; therefore, future hydrogen production must be largely carbon-free to be a credible lever for a sustainable future. Water electrolysis is the main process that can produce clean hydrogen on a large scale [13], as the electricity required for the process can be decarbonized (e.g., from renewable or nuclear sources). To promote the transition from gray/black to low-carbon hydrogen, the latter must be produced at a low cost.

One option currently being explored is the production of hydrogen from offshore wind turbines, as demonstrated by recent projects

* Corresponding author at: Mines Paris, PSL University, Centre for processes, renewable energy and energy systems (PERSEE), Sophia Antipolis, 06904, France.
E-mail addresses: antoine.rogeau@minesparis.psl.eu (A. Rogeau), robin.girard@minesparis.psl.eu (R. Girard).

¹ <https://www.lhyfe.com/>

² <https://aquaventus.org/>

³ <https://group.vattenfall.com/uk/what-we-do/our-projects/european-offshore-wind-deployment-centre/aberdeen-hydrogen>

Nomenclature	
Acronyms	
AHV	Anchor Handling Vessel
CTV	Crew-Transfer Vessel
EAR	Economically Attractive Resource
HLCV	Heavy-Lift Cargo Vessel
HVAC	High Voltage Alternating Current
HVDC	High Voltage Direct Current
JUV	Jack-Up Vessel
LCOH	Levelized Cost Of Hydrogen
O&M	Operation and maintenance
SOV	Service Offshore Vessel
SPIV	Self-Propelled Installation Vessel
SUBV	Self-Unloading Bulk Vessel
W2H	Wind-to-Hydrogen
W2P	Wind-to-Power
Subscripts and superscripts	
<i>BA</i>	Base
<i>C</i>	Cable
<i>CS</i>	Connection slots
<i>DS</i>	Desalination system
<i>EC</i>	Export cable
<i>EL</i>	Electrolyzer
<i>EP</i>	Export pipeline
<i>IA</i>	Inter-array
<i>IAP</i>	Inter-array pipeline
<i>inst</i>	Installation
<i>load</i>	Loading
<i>loss</i>	Losses
<i>maj</i>	Major
<i>MF</i>	Manifold
<i>misc</i>	Miscellaneous
<i>OP</i>	Offshore platform
<i>P</i>	Pipeline
<i>p</i>	Pipe
<i>PC</i>	Power converter
<i>PE</i>	Platform equipment
<i>PF</i>	Platform foundation
<i>PS</i>	Power Substation
<i>rep</i>	Repair
<i>s</i>	Stage
<i>SI</i>	Sand island
<i>TE</i>	Turbine equipment
<i>TF</i>	Turbine foundation
<i>unload</i>	Unloading
<i>WF</i>	Wind farm
<i>WT</i>	Wind turbine
Variables	
α	Multiplying factor (-)
\dot{V}_{H_2O}	Nominal flow rate (m^3/h)
\dot{v}_{H_2O}	Rated water consumption (m^3/MWh)
η	Efficiency (%)
λ	Failure rate (f/year)
A	Area (m^2)
BR	Bulk rate (m^3/h)
C	Rated cost ($\text{€}/\text{kW}$)
C_p	Capacitance (F/km)
$CAPEX$	Capital Expenditure
CD	Capacity density of wind farm (MW/km^2)
d	Diameter of pipe (m)
$DECEX$	Decommissioning Expenditure
DP	Distance to port (km)
DR	Day rate ($\text{€}/\text{day}$)
E	Energy (kg)
EC	Equipment cost (€)
f	Frequency (Hz)
h	Water depth (m)
I	Intensity (A)
IC	Installation cost (€)
L	Length of element (m)
l	Lifetime (y)
LC	Linear cost (€/m)
LIC	Linear installation cost (€/m)
LoC	Logistics cost (€)
MC	Maintenance cost (€)
N	Number of elements (-)
NL	Number of lifts (h)
$OPEX$	Operational Expenditure
P	Power (kW)
P^*	Equivalent electric power (kW)
R	Resistance (Ω)
r	Rate of return (%)
S	Section of cable (mm^2)
t	Time (h)
U	Tension (V)
UC	Unitary cost (€)
V	Volume (m^3)
VC	Vessel capacity (units/lift)

In addition, the cost of wind turbines and electrolyzers is expected to decrease in the next few years, thus offering a promising future for offshore wind projects.

1.2. Background

1.2.1. Offshore wind-to-power: Cost modeling and resource assessment

Offshore wind energy has been extensively studied in the past as it is considered a credible option for decarbonizing power generation. For this reason, some detailed cost modeling of offshore wind-to-power (W2P) projects has been published [15–18], often comparing high voltage alternating current (HVAC) and high voltage direct current (HVDC) power transmission to shore. In addition to the equipment costs for turbines, cables, and converters, additional costs can be considered depending on the level of detail and the focus of the studies, namely (1) installation costs [19–22], (2) operation and maintenance costs [22–24], and (3) decommissioning costs [22,25,26]. These modeling approaches have sometimes been specifically adapted, for example, for floating structures in deep waters [27–30].

Resource assessments are valuable tools for both stakeholders and energy modelers. Indeed, they permit not only to identify the most

(Lhyfe,¹ AquaVentus² or HT1³). Indeed, dedicated offshore wind-to-hydrogen (W2H) is expected to enable the development of far-from-shore wind projects [14], as they are less constraining to the use of the sea and offer the advantage of more constant and stronger winds.

economical locations to produce energy but also to estimate the global potential available within an area and the corresponding costs. Multiple resource assessments have been carried out in the past for W2P [31–33]. In particular, Martinez and Iglesias mapped the leveled cost of energy considering floating configurations in the European Atlantic [34] and in the Mediterranean Sea [35]. Beiter et al. [36] performed a similar assessment with a prospective focus on the United States. A site selection approach is also frequently developed to identify areas suitable for wind power projects [37–39]. Site selection and economic evaluation were sometimes coupled, e.g., by Caglayan et al. [40] and Hundleby and Freeman [41], the latter of whom produced economically attractive resource curves at European scale. Similar approaches have been used for other marine renewables such as wave energy [42].

It is worth noting that the modelings of costs used in resource assessment studies are often simplified, taking into consideration only part of all the expenditures presented above or adopting simplified models.

1.2.2. Offshore wind-to-hydrogen: A nascent field

In contrast, hydrogen production from offshore wind farms is a relatively new area of research. Some works summarized the current situation of W2H [43–45] and identified three main connection schemes for such projects, namely onshore, centralized offshore, and decentralized offshore electrolysis. Singlitico et al. [46] also considered these connection schemes for a study-case wind farm in the North Sea considering a parallel power-hydrogen export connection. Similarly, Lüth et al. [47] evaluated the most economical option between hydrogen and power connection for an energy island considering grid infrastructure and capacity expansion. Lucas et al. [48] estimated the economics of hybridizing an existing W2P project and analyzed the impact of electricity price fluctuations on the leveled cost of hydrogen (LCOH). Giampieri et al. [49] estimated the LCOH considering different energy carriers, such as hydrogen, electricity, and ammonia and analyzed the impact of hybridization on LCOH for a study-case wind farm. Kim et al. [50] studied three configurations of offshore wind farms for hydrogen generation and compared the LCOH for optimized sites and designs. Similarly, Jiang et al. [51] performed sizing optimization of offshore hydrogen generation wind farms but using simplified cost models. In all these works, no real site characteristics are considered and the wind farms configurations are theoretical.

Other works focus on energy transport, such as Miao et al. [52] and d'Amore Domenech et al. [53] which studied the economic evaluation of pipeline, barge, and power cable export options.

Some studies combine geographic analysis with economic evaluation of W2H projects. For instance, Komorowska et al. [54] conducted a case study in Poland that considers only onshore electrolysis. Dinh et al. [55] evaluated the LCOH of W2H projects in Ireland considering the centralized offshore connection scheme.

Finally, other studies are worth mentioning as they present similar analyses but for different ocean renewable energy: Serna and Tadeo [56] focused on wave energy, while Babarit et al. [57] considered a dedicated fleet of energy vessels.

1.3. Literature gaps and objectives of the paper

In view of the existing literature presented above, the following gaps are identified:

- The W2H costs of floating offshore wind projects have not been properly modeled, especially for the decentralized connection scheme
- There is no harmonized comparison of onshore electrolysis considering HVAC and HVDC export and offshore electrolysis including both centralized and decentralized options
- Few papers combine the cost modeling of wind turbines and electrolyzers, with projected costs

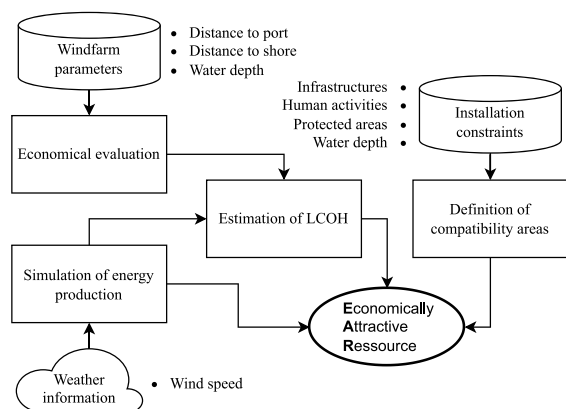


Fig. 1. Flowchart of the developed methodology.

- A global resource assessment, as has been published for W2P, has not yet been conducted, although it would allow the identification of the most economical sites and the overall potential of a study area

The objectives of this work are therefore threefold:

- Cost modeling review: The scattered cost models in the offshore wind and hydrogen production literature must be brought together into a detailed cost modeling that accounts for the effects of key on-site parameters (e.g. wind speed, water depth, distance to shore, and distance to port) and the different connection schemes for both onshore and offshore electrolysis
- Comparison of economics: The economics (e.g. the cost structure) of the different possible configurations for producing hydrogen from offshore wind is yet to be analyzed
- Resource assessment: A resource assessment must be carried out at European scale, taking advantage of the detailed cost modeling. Cost curves and a mapping of the best locations for offshore hydrogen production must then be generated

1.4. Methodology and paper outline

The LCOH is used to evaluate and compare the profitability of hydrogen production from offshore wind farms. LCOH is derived from lifetime costs and energy production over the lifetime of the project, as shown in Eq. (1).

$$LCOH = \frac{\sum_{t=0}^l \frac{CAPEX_t + OPEX_t + DECEX_t}{(1+r)^t}}{\sum_{t=0}^L \frac{E_t}{(1+r)^t}} \quad (1)$$

where *CAPEX*, *OPEX*, and *DECEX* represent the capital, operational, and decommissioning costs, respectively (€), *E* represents the energy produced or the amount of hydrogen produced (kg), *l* is the lifetime of the project (y), and *r* is the rate of return considered in the economic evaluation (%).

The steps required to perform the resource assessment are then threefold: (1) total lifetime costs and (2) energy production must be estimated at each site in the study area to determine the LCOH, while (3) suitable areas for offshore wind farm installation must be identified through a site selection process. The economically attractive resource (EAR), defined as the amount of energy that can be produced at a given price, can then be derived from the previous steps.

The global methodology is summarized in Fig. 1.

Consistent with the proposed methodology, the first section of this paper presents the connection schemes considered in this study before describing the detailed cost modeling in the second section. The third section describes the estimation of wind farm energy production, and

Table 1

Elements of the transmission chain for the different connection schemes as defined in Fig. 2. n is the number of wind turbines.

		Onshore	Offshore	
		Centralized	Decentralized	
Power substation	HVDC/HVAC offshore substation HVDC onshore substation	X		
Hydrogen production	Power converter Electrolyzers Desalinator Electrolysis platform	X	X X X	n .X n .X n .X
Transmission	Array cables Array pipelines Transmission cables Transmission pipeline	X X	X X	X

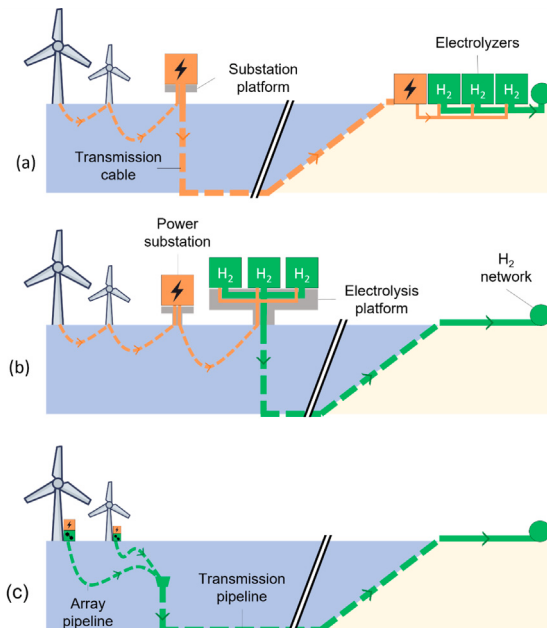


Fig. 2. Different connection schemes considered: (a) Onshore electrolysis (b) Centralized offshore electrolysis (c) Decentralized offshore electrolysis.

the fourth section presents the mapping procedure in detail. Finally, the fifth section applies the overall methods at European level and presents and discusses the results such as the mapping of LCOH, the generation of economically attractive resource curves, and the detailed cost structures. A conclusion summarizes the main findings and highlights the main perspectives.

2. Connection schemes considered

Water electrolysis can be carried out on shore – the electricity is transported to land via power cables – or directly offshore and then transported to land. In this work, we consider the transport of hydrogen via pipelines, although transport by tankers can be advantageous for very long distances (over 1000 km) [49,52,53].

We have defined three connection schemes for hydrogen production, which are represented in Fig. 2. The main elements of the conversion and transport chain of each configuration are listed in Table 1.

- Scheme 1 - onshore electrolysis:** The wind farm can be connected to the mainland by an HVDC or an HVAC power cable, depending on the distance [15–17]. In this case, hydrogen is produced by onshore electrolyzers. This configuration has the advantage of requiring a small offshore platform (only for the power conversion systems) but requires expensive subsea arrays and transmission cables, which also cause non-negligible power losses.

- Scheme 2 - centralized offshore electrolysis:** Hydrogen can also be produced directly offshore. Since electrolyzers are voluminous, they require their own platform. One option is to install the electrolyzers on a central platform in the wind farm. This configuration takes advantage of efficient, economical pipelines to transport hydrogen to shore.

- Scheme 3 - decentralized offshore electrolysis:** Another option for offshore production is to place an electrolyzer near each wind turbine. In this configuration, hydrogen is transported through individual inter-array pipelines between the turbines to a manifold before being sent onshore via a rigid pipeline. This configuration does not require the construction of massive platforms and incurs minimal losses and costs.

This study estimates the cost of producing hydrogen on the coastline. Potential additional costs for connecting to transportation infrastructures are not considered in this study.

3. Economic estimation of hydrogen production

To calculate the LCOH, we must first model *CAPEX*, *OPEX*, and *DECEX*. *CAPEX* comprises equipment costs, *EC*, and installation costs, *IC*, while *OPEX* includes material costs, *MC*, and logistics costs, *LoC*.

Element sizing is critical in calculating equipment costs, and losses at each stage of the hydrogen production chain (see Section 4.2) are considered to adjust sizing.

3.1. Equipment costs

3.1.1. Wind turbines

The cost of wind turbines can be divided into two elements, namely the turbine foundation, *TF*, and the turbine equipment, *TE*.

$$EC_{WT} = EC_{TE} + EC_{TF} \quad (2)$$

Fixed-bottom and floating wind turbines are considered, and turbine costs are the same for both configurations [58]. Both turbine and foundation costs are directly related to the number of turbines N_{WT} and their rated power P_{WT} (kW) over a rated cost RC (€/kW) as shown in Eqs. (3) and (4).

$$EC_{TE} = N_{WT} \cdot RC_{TE} \cdot P_{WT} \quad (3)$$

$$EC_{TF} = N_{WT} \cdot RC_{TF}(h) \cdot P_{WT} \quad (4)$$

The rated cost of the turbines is expected to decrease over the years, while the rated power of the wind turbines is expected to evolve in the opposite direction, reducing the number of wind turbines per wind farm and consequently the investment, installation, and operation costs. Corresponding hypotheses are presented in Table 2.

Regarding foundations, three options are considered:

- Monopile for shallow water, i.e., less than 25 meters deep
- Jacket for water depths between 25 and 55 meters

Table 2

Evolution of wind turbine costs and technical parameters.

Sources: [58,59].

	2020	2030	2050	
RC_{TE}	1500	1200	1000	(€/kW)
Rated power	8	15	20	(MW)

Table 3

Evolution of coefficients used for the foundation costs of wind turbines (see Eq. (5)). Sources: Estimations based on [58] and [59].

		Turbine foundation		
		Monopile	Jacket	Floating
2020	c_1	201	114	0
	c_2	613	-2270	774
	c_3	812	932	1481
2030	c_1	181	103	0
	c_2	552	-2043	697
	c_3	370	478	1223
2050	c_1	171	97	0
	c_2	521	-1930	658
	c_3	170	272	844

- Floating for waters deeper than 55 meters

The modeling of the rated cost of the foundations is based on Bosch et al. [58], and depends on the water depth, h (m), as shown in Eq. (5).

$$RC_{TF}(h) = c_1 \cdot h^2 + c_2 \cdot h + c_3 \cdot 10^3 \quad (5)$$

The coefficients c_1 , c_2 , and c_3 differ by foundation type and decrease with time, as shown in Table 3. The coefficient values of Bosch et al. [58] were adjusted to match the projections of RTE [59]. Depending on the water depth and installation year, foundation costs account for between 16% and 60% of the total wind turbine cost.

In the case of decentralized offshore electrolysis, the foundation of the wind turbines must be adapted to accommodate the electrolyzers (e.g., by adding a dedicated platform [44,46]). Since the cost of the foundation is determined by the weight to be supported, this change is modeled by an additional cost set at 20% of the cost of the foundation, since the power density of the electrolyzers is estimated to be 20% of the power density of the wind turbine (based on manufacturers' data and our own estimates).

3.1.2. Offshore platforms

Offshore electrolyzers and power substations require a dedicated platform. Offshore platform costs are modeled similarly to wind turbines (see Section 3.1.1), and include the cost of platform equipment, PE , and platform foundations, PF .

$$EC_{OP} = EC_{PE} + EC_{PF} \quad (6)$$

EC_{PE} depends on the equipment installed and is defined later in this article (see Section 3.1.3 for substations and Section 3.1.4 for electrolysis plants).

Depending on the water depth at the site, three types of platforms can be constructed to accommodate the equipment:

- Sand islands are used in shallow waters (below 30 m depth) because they significantly reduce investment costs as the size of the wind farm increases. For this reason, they are planned for energy hubs in the North Sea [46]
- Jacket platforms are being considered for deeper waters (up to 150 m)
- Floating platforms are required for deep seas (over 150 meters deep)

Table 4

Cost parameters of sand islands.

Source: [46].

$C_{SI,V}$	3.26	(€/m ³)
$C_{SI,A}$	804.00	(€/m ²)

Table 5

Evolution of coefficients used for the foundation costs of platforms.

Sources: Estimations based on [61,62].

	Platform foundation	
	Jacket	Floating
RC	c_2	233
	c_3	47
UC	c_2	309
	c_3	62

Table 6

Cost parameters of HVDC and HVAC substations.

Source: [16,46,63,64].

	HVDC	HVAC
RC_{PS}	102.93	22.87
UC_{PS}	31.75	(€/kW) (M€)

3.1.2.1. Sand island. The cost of a sand island EC_{SI} , presented in Eq. (7), depends on the volume of sand V_{SI} (m³) and the area to be protected A_{SI} (m²), defined by Singlito et al. [46]. For substations and electrolyzers, a footprint of 5 m²/MW and 20 m²/MW, respectively, is assumed [46,60]. The cost hypotheses are presented in Table 4.

$$EC_{SI} = C_{SI,V} \cdot V_{SI}(h) + C_{SI,A} \cdot A_{SI}(h) \quad (7)$$

3.1.2.2. Jacket and floating platforms. The modeling of foundation costs – presented in Eq. (8) – is based on the cost modeling of turbine foundations (see Eq. (4)). The dependence on water depth is simplified to a piecewise linear function and calibrated to match literature values [34,46,61,62]. The coefficients used to estimate the rated and unit costs of foundations (RC_{PF} and UC_{PF}) are presented in Table 5.

$$EC_{PF} = RC_{PF}(h) \cdot P_{WF}^* + UC_{PF}(h) \quad (8)$$

Due to the novelty of dedicated electrolysis platforms, no cost data or models are available in the literature, so the cost data obtained are mostly for platforms with substations. Therefore, foundation costs are expressed as a function of equivalent electrical power P_{WF}^* . Based on manufacturers' data and our own assumptions, HVDC substations are assumed to have twice the power density (in W/kg) of electrolyzers and half the power density of HVAC platforms [16,34], and so P_{WF}^* is calculated using Eq. (9).

$$P_{WF}^* = \begin{cases} P_{WF} & \text{if HVDC substation,} \\ 0.5 \cdot P_{WF} & \text{if HVAC substation,} \\ 2 \cdot P_{WF} & \text{if electrolysis plant.} \end{cases} \quad (9)$$

3.1.3. Power substation

The equipment costs of power substation EC_{PS} depend on the capacity of the wind farm and the type of substation (HVAC or HVDC), as shown in Eq. (10).

$$EC_{PS} = RC_{PS} \cdot P_{WF} + UC_{PS} \cdot 10^3 \quad (10)$$

The substation cost hypotheses are presented in Table 6.

3.1.4. Electrolysis plant

3.1.4.1. Electrolyzers. Electrolyzer costs are expected to radically decrease in cost by 2050, making green hydrogen more affordable [13]. Proton exchange membrane electrolyzers are the preferred option for

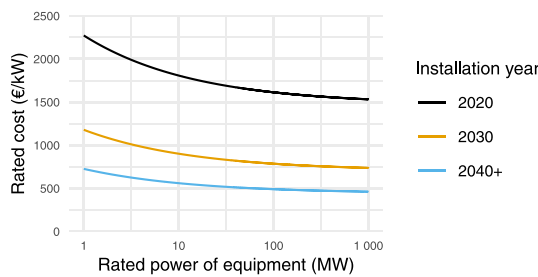


Fig. 3. Evolution of electrolyzer-rated costs with time.
Source: Adapted from [66].

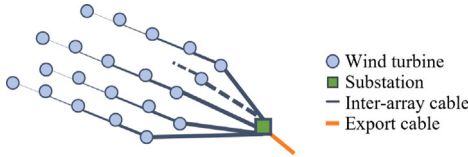


Fig. 4. Schematic string-based layout considered for wind farms in onshore and centralized offshore electrolysis configurations. The electrolyzers are located on the platform or onshore.

Table 7
Cost parameters of electrolysis systems.
Source: [66].

k_0	673.73	(€)
k	10,876.93	(€)
α	0.662	–
Y_0	2020	–
β	-104.45	–

offshore production because they produce hydrogen at higher pressure and require limited footprint and operating temperature [46,65]. The equipment cost for electrolyzers EC_{EL} is given by Eq. (11), taking into account a scaling effect and a learning rate [66].

$$EC_{EL} = RC_{EL} \cdot P_{EL} \quad (11)$$

where

$$RC_{EL} = (k_0 + k \cdot p_{EL}^{\alpha-1}) \cdot \left(\frac{Y}{Y_0} \right)^\beta + RC_0 \quad (12)$$

where k_0 and k are constants, P_{EL} is the rated power of the electrolyzer (kW_e), and Y and Y_0 are the installation year and reference year, respectively. RC_0 is an additional fixed cost representing the electrolyzer-to-system cost (connection, sealing, etc.), which decreases over time and is defined to be consistent with literature values [60,64]. These costs double if the electrolyzer is at sea [46].

Fig. 3 represents the evolution of the cost of the electrolyzer as a function of the rated power of the system for the years 2020, 2030, and after 2040, taking into account the parameter values listed in Table 7.

The maximum rated power of electrolyzers is expected to increase in the coming years. In 2022, the maximum rated capacity is expected to be 20 MW, increasing to 200 MW by 2050. If necessary, multiple electrolyzers will be installed to reach the wind farm's total capacity.

3.1.4.2. Power converter. Since wind turbines supply AC power while electrolyzers require DC power, offshore production systems require power converters and circuit breakers, and the cost of power conversion EC_{PC} (€) is calculated using Eq. (13). The corresponding cost hypotheses can be found in Table 8 [64].

$$EC_{PC} = RC_{PC} \cdot P_{PC} \quad (13)$$

Table 8
Cost parameters of conversion elements.

Source: [46,68].

RC_{PC}	104.13	(€/kW)
RC_{DS}	30.56	(€/m ³)
\dot{v}_{H_2O}	263	(m ³ /kW)

Table 9

Technico-economic assumptions for inter-array cables.

Sources: [63,69–72] and own assumptions.

<i>i</i>	Tension (kV)	Section (mm ²)	Resistance (Ω/km)	Capacity (MW)	Cost dynamic (€/m)	Cost static (€/m)	Inst. cost (€/m)
1	66	95	0.25	24	180	113	113
2		150	0.16	30	215	134	121
3		300	0.08	42	298	186	149
4		400	0.06	49	357	223	156
5		630	0.04	59	456	285	171
6		800	0.03	69	577	361	180
1	132	120	0.2	80	288	152	114
2		150	0.16	87	358	188	122
3		300	0.08	123	747	393	216
4		400	0.06	136	900	474	213
5		630	0.04	162	1228	646	226
6		800	0.03	201	1779	936	281

3.1.4.3. Desalinator. Offshore hydrogen production requires seawater desalination to obtain the large amount of freshwater needed for electrolysis. The cost of the desalination system EC_{DS} is estimated using Eq. (14) [46].

$$CAPEX_{DS} = RC_{DS} \cdot \dot{v}_{H_2O} \quad (14)$$

where RC_{DS} is the rated cost of the desalinator (€/(m³/h)) and \dot{v}_{H_2O} is the nominal flow rate of water (m³/h).

The desalinator is sized at 80% of the electrolyzers P_{EL} rated power (kW), taking into account a small buffer tank for fresh water. The nominal flow rate of water is then related to the rated power of the electrolyzer by Eq. (15), where the nominal water consumption of the electrolyzers \dot{v}_{H_2O} is estimated to be 0.263 m³/MWh [67].

$$\dot{v}_{H_2O} = \dot{v}_{H_2O} \cdot 0.8 \cdot P_{EL} \quad (15)$$

3.1.5. Inter-array connection

3.1.5.1. Electric inter-array connection. With the exception of the decentralized offshore configuration, the electricity generated by the wind turbines is transmitted to a substation through inter-array cables. The investment cost of the inter-array cables EC_{IA} depends on the length and cross-section of the cables. A string-based layout is considered, shown in Fig. 4, and the cable cross-section S increases along the array within its capacity limit. The total inter-array cost is estimated using Eq. (16).

$$EC_{IA} = N_A \cdot \left(\sum_i LC_{S_i} \cdot L_{S_i} + LC_{S_{max}} \cdot L_{S_{max,HUB}} \right) \quad (16)$$

where N_A is the number of arrays needed, and LC_{S_i} and L_{S_i} are the linear cost (€/m) and the total length (m) of the inter-array cables of section S_i , respectively. S_{max} is the largest cable section needed and $L_{S_{max,HUB}}$ is the length of cable needed to connect the arrays to a sand island hub if needed (see Section 3.1.2.1).

The techno-economic parameters of the inter-array cables are shown in Table 9. Both 66 kV and 132 kV cables are considered, since the rated tension increases with the rated power of the turbines.

The cable length of the section S_i is calculated as in Eq. (17). The number of wind turbines connected to this section N_{S_i} depends on the remaining available capacity considering the wind turbines connected to the upstream sections. We limited the number of turbines per array to 8 to limit power losses.

$$L_{S_i} = N_{S_i} \cdot L_{IA} \quad (17)$$

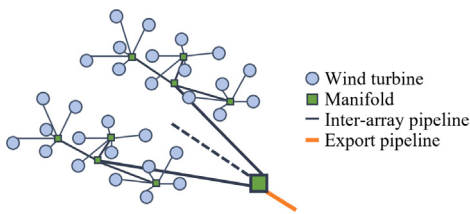


Fig. 5. Schematic radial layout considered for wind farms in a decentralized offshore electrolysis configuration. An electrolyzer is located in each wind turbine.

$$\text{with } N_{S_i} = \left\lfloor \frac{P_{S_i} - \sum_{k=1}^{i-1} N_{S_k} \cdot P_{WT}}{P_{WT}} \right\rfloor$$

where L_{IA} is the length of the inter-array cable between two turbines (m) and is calculated according to Eq. (18) [73]. The mean distance between two turbines $D_{WT} = \sqrt{\frac{P_{WT}}{CD_{WF}}}$ depends on CD_{WF} and P_{WT} , the capacity density (MW /km²) and the rated power (MW) of the wind turbines, respectively.

$$L_{IA} = 2 \cdot 2.6 \cdot h + D_{WT} \quad (18)$$

At water depths greater than 200 m, laying the inter-array cables on the seabed is not economical and they are suspended [74,75]. To ensure continuity of LCOH at this boundary, the failure rate (see Section 4.3) of suspended cables is considered 10% higher than that of laid cables.

When connecting to a sand island, the required length of static cable is estimated using the formula presented in [46]. Otherwise, the arrays are connected to a centralized platform, and the additional cable length $L_{S_{max,HUB}}$ is equal to D_{WT} .

3.1.5.2. Pipeline inter-array connection. In the case of decentralized production (i.e., one electrolyzer in each turbine), the hydrogen is collected by flexible pipes connected to the transport pipe via manifolds, as shown in Fig. 5. The manifolds have a limited number of connection slots N_{CS} which means that the manifolds are cascaded into N_s connection stages, as calculated by Eq. (19).

$$N_s = \lceil \log_{N_{CS}}(N_{WT}) \rceil \quad (19)$$

For each stage i , the required length of pipes is estimated using Eq. (20), which depends on the number of pipes N_p connected to each of the $N_{MF,i}$ manifolds in that stage i and A_i the total area covered by the downstream wind turbines (km²). The first pipe stage (from the turbines to the seabed) consists of flexible pipes, while rigid pipes are used in the other stages.

$$L_i = \begin{cases} N_{WT} \cdot \left(\frac{\sqrt{A_i}}{\sqrt{2}} + h \right), & \text{if } i = 1 \\ N_p \cdot N_{MF,i} \cdot \frac{\sqrt{A_i}}{\sqrt{2}}, & \text{otherwise} \end{cases} \quad (20)$$

The cost of inter-array pipeline equipment costs EC_{IAP} is then calculated by Eq. (21).

$$EC_{IAP} = \sum_{i=1}^{N_s} \left(\alpha_s(d_i) \cdot LC_{BA,IAP} + LC_{misc,IAP}(d_i) \right) \cdot L_i \quad (21)$$

where $\alpha_s(d)$ and $LC_{misc}(d)$ are a size factor and miscellaneous cost (for more details and values, see [76]) and LC_{BA} is the base cost of flexible pipes (€/m) defined in Table 10.

The diameter of the pipeline at stage i (d_i (m)) is recursively calculated based on the diameter of the export pipeline (see Eq. (29)), as defined in Eq. (22). A minimum diameter of 5 cm is considered.

$$d_i = \max \left(0.05, \frac{d_{i-1}}{\sqrt{N_c}} \right) \quad (22)$$

Manifolds connect pipes in groups and then to the transmission pipeline. The cost model is similar to that for inter-array pipelines in

Table 10

Main parameters values used for pipes (flexible and rigid) and manifold costs estimation.

Source: [76].

N_{CS}	5	(slots)
LC_{BA}	1736.73	(€/m)
	173.67	(€/m)
UC_{BA}	2.265	(M€)
$UC_{misc,MF}$	0.188	(M€)

that it depends on the diameter of the connected pipelines. In this work, we assume that each manifold has 5 connection slots, except for the last manifold, which may have fewer slots. The total cost of manifolds EC_{MF} is expressed by Eq. (23).

$$EC_{MF} = \sum_{i=1}^{N_s} \left(\alpha_s(d_i) \cdot \alpha_N(N_{CS}) \cdot UC_{BA,MF} + UC_{misc,MF} \right) \cdot N_{MF,i} \quad (23)$$

where $\alpha_s(d)$ and $\alpha_N(N_{CS})$ are factors that depend on the pipe diameter and the number of connection slots, respectively. For more details and values, see [76]. UC_{BA} and UC_{misc} are the base and miscellaneous costs (€), respectively, defined in Table 10.

3.1.6. Energy export

As a conservative assumption, the total length L of the export cable or pipeline is assumed to be 1.2 times the distance to shore DS_{WF} .

$$L = 1.2 \cdot DS_{WF} \quad (24)$$

An export cable is required for the onshore electrolysis scheme. Both HVAC and HVDC export cables are considered, since the most economical solution depends mainly on the distance to the coast, with the break-even point at a transport distance of about 50–80 km [15–17]. For the offshore electrolysis scheme, an export pipeline is considered.

3.1.6.1. HVDC cable. The investment cost of the HVDC export cable $EC_{EC,HVDC}$ is described by Eq. (25).

$$CAPEX_{EC,HVDC} = RC_{EC,HVDC} \cdot P_{EC,HVDC} \cdot L_{EC} \quad (25)$$

where $RC_{EC,HVDC}$ is the linear cost of the cable estimated at 1.35 €/W/km [18,71], $P_{EC,HVDC}$ is the rated power of the export cable (MW) and L_{EC} is the length of the export cable.

3.1.6.2. HVAC cable. The power capacity of HVAC cables decreases nonlinearly with distance, so as the distance from the coast increases, the cross-section of HVAC cables must be reduced and multiple cables must be laid in parallel [15].

The cables considered in this study are shown in Table 11.

The power capacity of the cable P_{EC} (W) is given by Eq. (26) [15] and the appropriate cable cross-section and rated voltage are selected to minimize the number of cables $N_{EC,HVAC}$ and thus the cost.

$$P_{EC} = \sqrt{(\sqrt{3} \cdot U \cdot I)^2 - (\frac{1}{2} \cdot U^2 \cdot 2\pi \cdot f \cdot C_p \cdot L_{EC})^2} \quad (26)$$

where U is the cable voltage (V), I is the ampacity of the cable (A), f is the frequency, which is assumed to be 50 Hz, and C_p is the capacitance (F/km).

The equipment cost of the HVAC export cables $IC_{EC,HVAC}$ is then calculated using Eq. (27).

$$EC_{EC,HVAC} = N_{EC,HVAC} \cdot LC_{EC,HVAC} \cdot L_{EC} \quad (27)$$

where $LC_{EC,HVAC}$ is the linear cost of the cable (€/m) given in Table 11.

Table 11

Techno-economical assumptions for HVAC export cables.

Sources: [15,69–72] and own assumptions.

Tension (kV)	Section (mm ²)	Resistance (mΩ/km)	Capacitance (nF/km)	Ampacity (A)	Cost (€/m)	Inst. Cost (€/m)
132	630	39.5	209	818	406	335
	800	32.4	217	888	560	340
	1000	27.5	238	949	727	350
220	500	48.9	136	732	362	350
	630	39.1	151	808	503	360
	800	31.9	163	879	691	370
	1000	27.0	177	942	920	380
400	800	31.4	130	870	860	540
	1000	26.5	140	932	995	555
	1200	22.1	170	986	1130	570
	1400	18.9	180	1015	1265	580
	1600	16.6	190	1036	1400	600
	2000	13.2	200	1078	1535	615

3.1.6.3. Rigid pipeline. If the electrolyzers are located offshore, the generated hydrogen must be transported to shore via an export pipeline. The same cost modeling is used for the export pipeline as for the inter-array pipes (see Section 3.1.5.2) as presented in Eq. (28).

$$EC_{EP} = \left(\alpha_s(d) \cdot LC_{BA,EP} + LC_{misc,EP}(d) \right) \cdot L_{EP} \quad (28)$$

As for inter-array pipes, the cost coefficients are presented in Table 10, and rigid pipes are considered for export.

The diameter of the export pipeline increases with distance from the coast and the power of the wind farm, since more hydrogen must flow through the pipeline and the pressure drop is significant [44]. Eq. (29) models the evolution of the export pipeline diameter d_{EP} (m).

$$d_{EP} = 0.200 + 0.346 \cdot 10^{-3} \cdot L_{EP} + 0.065 \cdot P_{EP} \cdot 10^{-9} \quad (29)$$

where L_{EP} is the length of the pipeline (m).

3.2. Installation costs

3.2.1. Wind turbines

A simplified version of the modeling developed by Kaiser and Snyder [20] is used in this paper. Installation costs depend on:

- The characteristics of the vessel needed to transport the turbines (speed, capacity, and daily rate)
- The time and equipment required to install the turbines on site

The general installation cost for wind turbines IC_{WT} (€) is calculated as shown in Eq. (30).

$$IC_{WT} = \left(NL \cdot \left(\frac{2 \cdot DP_{WF}}{v} + t_{load} \right) + t_{inst} \cdot N_{WT} \right) \cdot \frac{DR}{24} \quad (30)$$

where $NL = \frac{N_{WT}}{VC_b}$ is the number of lifts required, VC_b is the vessel capacity (units/lift), DP_{WF} is the distance to the nearest port (km), v the speed of the ship (km/h), t_{load} the loading time of each lift (h), t_{inst} the installation time of the wind turbine (h), and DR the day rate of the ship (€/d).

Fixed wind turbines are transported by a self-propelled installation vessel (SPIV), which provides both transport and installation of turbines and foundations. The number of turbines transported per lift depends on their rated power, and the vessel capacity is set at 40 MW /lift. The number of lifts must be doubled, as foundations must also be transported and installed.

Floating wind turbines are assembled onshore and then towed by tugs to the farm site, where they are moored by special vessels called anchor handling vessels (AHVs). Three tugboats are needed to transport a floating wind turbine, while a single AHV can moor 7 of them.

Table 12 summarizes the input parameters.

Table 12

Parameters of the vessels used for wind turbine installation.

Sources: [19,20,27,29,77,78].

	Vessel	Capacity	Speed	Fixed	Floating
				Trans.	Ancho.
Vessel		SPIV		Tug	AHV
Capacity	<i>VC</i>	^a		0.3	7
Speed	<i>v</i>		18.5	7.5	18.5
Load. time	<i>t_{load}</i>		24	5	(h/lift)
Inst. time	<i>t_{inst}</i>		144	–	(h/u)
Dayrate	<i>DR</i>		200	2.5	(k€/d)

^a Depends on the rated power of turbines.

Table 13

Parameters of the vessels used for platform installation.

Sources: [20,29].

	Vessel	Capacity	Speed	Fixed	Floating
				Trans.	Ancho.
Vessel		SPIV		HLCV	AHV
Capacity	<i>VC</i>	1		1	3
Speed	<i>v</i>	18.5		22.5	18.5
Load. time	<i>t_{load}</i>		24	10	(h/lift)
Inst. time	<i>t_{inst}</i>		96	–	(h/u)
Dayrate	<i>DR</i>		200	40	(k€/d)

Table 14

Parameters of the vessels used for sand island construction.

Source: Own assumptions.

	Sand island	
Vessel		SUBV
Capacity	<i>VC</i>	20,000 (m ³ /lift)
Speed	<i>v</i>	25 (km/h)
Load. rate	<i>BR_{load}</i>	2000 (m ³ /h)
Unload. rate	<i>BR_{unload}</i>	6000 (m ³ /h)
Dayrate	<i>DR</i>	15 (k€/d)

3.2.2. Platforms

Fixed platforms are installed with SPIVs, similar to fixed wind turbines. Floating substations require heavy-lift cargo vessels (HLCVs). The input parameters are contained in Table 13.

Sand island installation requires sand to be loaded, transported, and unloaded at the farm site using self-unloading bulk vessels (SUBVs). Sand island installation costs IC_{SI} are estimated using Eq. (31) and input parameters are summarized in Table 14.

$$IC_{SI} = \left(\frac{V_{SI}}{VC_{SUBV}} \cdot \frac{2 \cdot DP_{WF}}{v_{SUBV}} + \frac{V_{SI}}{BR_{load}} + \frac{V_{SI}}{BR_{unload}} \right) \cdot \frac{DR}{24} \quad (31)$$

3.2.3. Cables and pipes

The installation costs of cables are modeled by linear costs representing the expenses of laying and burying [71], as shown in Eq. (32).

$$IC_C = LIC_C \cdot L_C \quad (32)$$

, where LIC is the linear installation cost of the cable (€/m), which takes into account the laying and burial costs, and L_C is the length of the cable to be laid (m). The values of the installation costs of inter-array cables and HVAC export cables are given in Table 9 and Table 11, respectively. For HVDC export cables, installation costs are included at 50% of the equipment cost [71].

Pipe installation costs are modeled by considering that Flex-lay or S-lay vessels are required for infield and export pipelines, respectively. Pipe installation costs IC_{CP} are calculated according to Eq. (33) and the corresponding inputs are listed in Table 15.

$$IC_P = \frac{L_{EP}}{LR} \cdot DR \quad (33)$$

Table 15

Parameters of the vessels used for pipeline installation.

Sources: Adapted from: [79–82].

Vessel	Pipeline			
	IA	Exp.		
Lay. rate	Flex	S-Lay		
Dayrate	LR DR	7.0 400	4.0 700	(km/d) (k€/d)

Table 16

OPEX values of power chain elements, defined as a share of the equipment costs.

Sources: [46,64,83].

	MC (% EC)
Wind turbines	2.5%
Sand island	1.5%
HVDC/HVAC substation	1.5%/3% ^a
Electrolyzers	2%/4% ^a
Power converters	1%/2% ^a
Desalinator	3%
Power cables	0.2%
Pipelines	2%

^a Onshore/offshore values.

3.3. OPEX

Operation and maintenance (O&M) costs depend primarily on the need for spare parts, but also increase with distance from the port, as vessels must reach the wind farm.

The O&M costs are determined by two elements: The material costs MC (€), which consist of the replacement of equipment parts, and the logistics costs LoC (€). In addition, the energy losses during conversion and transport can be included in the operating costs.

3.3.1. Repair costs

The repair costs of the different elements of the hydrogen production chain, defined as a percentage of the equipment costs, are shown in Table 16.

3.3.2. Logistics costs

Logistics costs correspond to the cost of reaching the turbines for maintenance using specialized vessels.

Minor repairs are performed with light vessels. An onshore-based strategy with crew transfer vessels (CTVs) can be used if the farm is located near the coast. A mothership-based strategy using service offshore vessels (SOVs) is more suitable for large parks or parks far from the coast, as it avoids very long trips and increases turbine availability [24,84–86].

The considered maintenance strategy guarantees a wind farm availability of 94%, as observed in many existing cases [87,88]. Logistics costs are modeled as increasing linearly up to 150 km from shore, where a SOV strategy stabilizes costs, as shown in Fig. 6.

Major repairs require more extensive intervention, and maintenance of fixed wind turbines is performed *in situ* using a jack-up vessel (JUV), while floating wind turbines must be towed to port or to an assembly site for repair [23].

The annual logistics cost for major repairs LoC_{maj} is calculated using Eq. (34), where the corresponding parameters are shown in Table 17.

$$LoC_{maj} = N_{WT} \cdot \lambda_{maj} \cdot \left(\frac{2n \cdot DP_{WF}}{v} + t_{rep} \right) \cdot \frac{DR}{24} \quad (34)$$

where λ_{maj} is the failure rate, assumed to be 0.08 failures per year [84], and n is the number of round trips required for major maintenance.

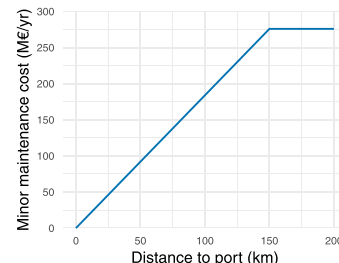


Fig. 6. Evolution of minor maintenance costs of wind turbines and conversion equipment.

Sources: Adapted from [84,86,89].

Table 17

Parameters of the vessels used for major wind turbine repairs.

Sources: [23,84].

Vessel	Fixed	Floating	–	
	JUV	Tug		
Speed	v	18.5	7.5	(km/h)
Repair time	t_{rep}	50	50	(h)
Dayrate	DR	150	2.5	(k€/d)
Roundtrips	n	1	2	–

Table 18

Decommissioning times or removal rates.

Sources: [26].

	Decom. time /Removal rate	
Fixed turbine	144	(h)
Anchors	30	(h)
Fixed platform	96	(h)
Export pipeline	5	(km/d)
IA pipeline	10	(km/d)

Table 19

Loss values along the hydrogen transmission chain .

Sources: [49,64,91].

	Losses
HVAC cables	^a
HVDC cables	3.0 (%)
Pipes	0.03 (%/1000 km)

^a Depend on the flowing power, calculated below.

3.4. DECEX

The decommissioning operations are very similar to the installation processes. For simplicity, the cost structure for decommissioning is considered the same as for installation, but the dismantling times are significantly lower. The considered times for decommissioning elements are given in Table 18. Decommissioning costs equal to half of the installation costs are applied to the inter-array and export cables.

4. Energy production

4.1. Wind power production

The power generation is derived from the wind speed by the theoretical power curves of the wind farm, shown in Fig. 7. The power curves evolve based on the tendency to increase the swept area of the wind turbines to generate power at lower wind speeds [90].

4.2. Energy losses

Energy losses occur at each step of the hydrogen production chain and reduce the final energy production. These losses can occur during

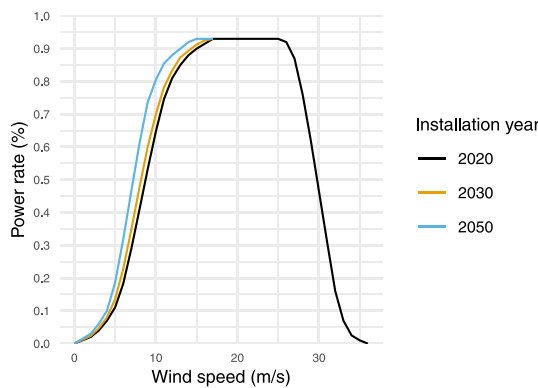


Fig. 7. Wind farm power curves considered for the different installation years.
Sources: [90].

Table 20
Efficiency values along the hydrogen production chain.
Sources: [13,49,60,64,91].

	Efficiency
HVDC substation	99%
Power converters	99.5%
Electrolyzers	62%
2020	65%
2030	70.5%
2050	70.5%
Desalinator	99.9%

Table 21
Failure rates and repair times considered for cables and pipelines.
Sources: [92,93].

		Failure rate (f/yr/km)	Repair time (d)
Cable	HVAC	0.003	40/60 ^a
	HVDC	0.0015	60
Pipeline	Flexible	0.001	40
	Rigid	0.0001	60

^a Repair time for inter-array and export cable respectively.

transmission (see [Table 19](#)) or conversion (see [Table 20](#)). The specific energy consumption of a desalination plant is about 4 kWh/m³ [68], which is about 0.1% of the electrolyzer consumption. HVAC cable losses (IA and export) are estimated for the whole year and are shown in Eq. (35) [69].

$$\eta_{HVAC} = 1 - \sum_t \frac{P_{loss}(t)}{P_{prod}(t)} \quad (35)$$

with $P_{loss} = \left(\frac{P_{prod}(t)}{U} \right)^2 \cdot R \cdot L$

where $P_{prod}(t)$ is the power flowing through the cable at time t , and R is the linear resistance as defined in [Table 9](#). Losses are calculated section by section along the array cables and along the export cable.

4.3. Failure rates and unavailability of the wind farm

If a failure occurs somewhere in the production, conversion, or transmission steps, some production is lost because part or all of the wind farm is unavailable. As shown in [Section 3.3.2](#), maintenance costs are modeled to ensure a global availability of 94% of wind turbines and electrolyzers.

Power cables and pipelines may also experience failures that result in full or partial unavailability of production; the longer the connection, the higher the failure rate. The failure rates and repair times considered are shown in [Table 21](#).

5. Mapping of the resource

The economic modeling presented above is used to estimate the European economically attractive resource of hydrogen from offshore wind energy. For this purpose, site selection must be performed before the site-specific costs of hydrogen production systems at each site can be estimated.

5.1. Site selection

The site selection problem has been extensively studied in the past in both academic literature [37,38] and technical reports [41]. Therefore, the methodology developed in this work to identify suitable zones for WP development is not presented in detail.

Following the methodology of Hundley and Freeman [41], we considered four levels of restriction with four associated wind farm densities:

- General: No particular restriction, maximum wind farm coverage set at 56% to leave room for vessel movement and wake effects
- Sensitive: Minor restrictions, reducing maximum coverage by 20% and setting it at 45%
- Very Sensitive: Major restrictions, implying sparser wind farms. Maximum coverage reduced by 50% and set at 28%
- Exclusion: Wind farms cannot be built

The constraints considered are detailed in [Table 22](#) along with the thresholds defined. Two new user-defined constraints are considered and derived from global datasets. Maritime routes are derived from EMODnet data [94], with routes considered dense (or medium) if more than 1000 trails per square meter per year are observed (or 500). Fishing effort data are provided by Global Fishing Watch based on data from AIS [97]. The Exclusion threshold considered (or Very Sensitive and Sensitive) corresponds to the 5% most heavily fished waters (or 10% and 20%).

5.2. LCOH estimation at European scale

To estimate the LCOH at European level, the following four inputs are provided as geographic information:

- Distance to coast: The coastline, excluding small islands, is used to calculate the shortest distance to the coast
- Distance to ports: Ports of size M and L from the World Port Index [100] are considered suitable for offshore activities. The distance to the port is calculated based on a grid distance while avoiding land
- Depth: Bathymetric information from EMODnet is used [96]
- Wind speed: Eleven years (2010–2020) of ERA –5 hourly wind speed at 100 m [98] are used for the analysis as this database is reliable for offshore wind assessment [101]

For this study, the installed capacity of wind farms was set to 1 GW with a capacity density of 6 MW /km², in agreement with observed values [102,103]. Finally, a lifetime of 25 years and a rate of return of 5% are considered. The resolution of all datasets is set to 5 × 5 km to be compatible with the large scale of the resource assessment.

6. Results and discussion

6.1. Resource assessment

6.1.1. Mapping of the resource

Lifetime costs, LCOH and energy potential are estimated for the whole European marine area. The results of the assessment are visualized as maps in [Fig. 8](#) showing annual energy and LCOH over Europe in 2030. Iceland is excluded from the assessment as the country is unlikely to participate in a European hydrogen market.

Table 22

Constraints considered for the identification of suitable zones and thresholds defined for the four restriction levels.

Sources: [39,41].

			Exclusion	Very sensitive	Sensitive	General	Data
Distance	Maritime routes (m)	Dense	< 3500			> 3500	[94]
		Medium	< 1500			> 1500	[94]
	Power cables (m)		< 500		< 1500	> 1500	[94]
	Telecom. cables (m)		< 500		< 1500	> 1500	[94]
	Existing wind farms (km)		< 8			> 8	[94]
	Shore (km)		< 10		< 20	> 20	[95]
	Depth (m)		> 1000				[96]
	Fishing effort (h/km ² /yr)		> 24.6	> 14.5	> 6.7	< 6.7	[97]
	Wind power density (W/m ²)		< 500				[98]
	Human activities			Aggregate extr. Munitions			[94]
Exclusion zones	Protected areas		IUCN Ia - III		IUCN IV - VI		[99]
					Natura 2000		[99]
					RAMSAR		[99]

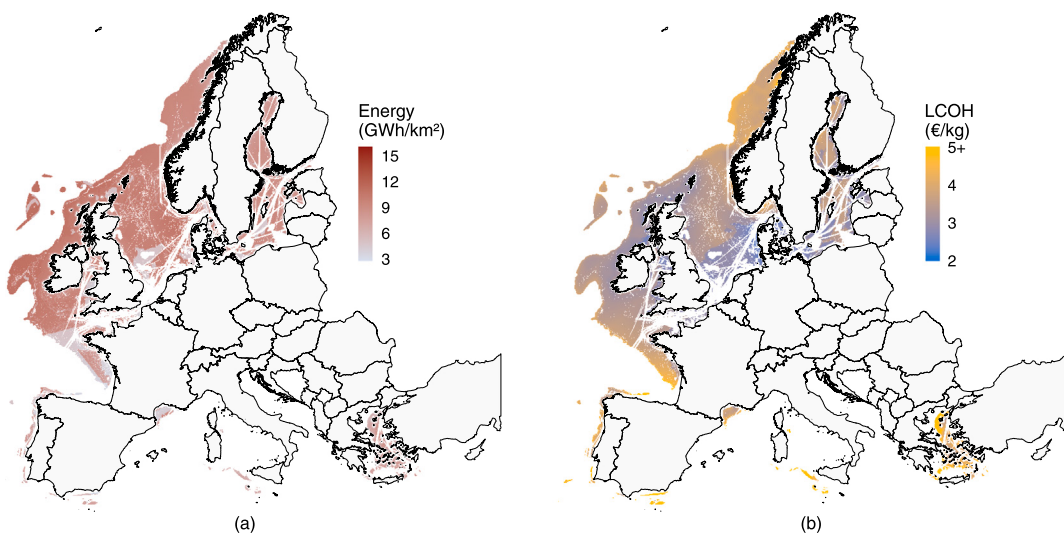
**Fig. 8.** European maps of European (a) yearly energy production and (b) LCOH in 2030.

Fig. 8(a) provides a visual representation of constraints on wind projects. About 43% of European seas are unavailable due to depths greater than 1000 m, 34% are excluded due to technical or environmental constraints as defined in Section 5.1, and about 7% are subject to non-exclusive constraints. The latter areas are characterized by lower annual energy production, shown in gray on the map.

The North Sea and waters near the United Kingdom and Ireland are identified on **Fig. 8(b)** as areas where large quantities of hydrogen can be produced at low LCOH. In contrast, the Mediterranean Sea offers limited resources of expensive hydrogen.

6.1.2. Economically attractive resource

The European potential can be represented as a merit order ranked by LCOH. These curves are drawn from 2020 to 2050, shown in **Fig. 9**. The potential grows over time—from about 10,000 TWh/year in 2020 to 13,750 TWh/year in 2050—due to increases in the efficiency of electrolyzers and the swept area of turbines. These potentials are enormous compared to hydrogen consumption in Europe in 2020 (339 TWh [10]) and in 2050 (664 to 4000 TWh [12]). In the theoretical case where all European hydrogen is produced by W2H projects, the most expensive hydrogen would range from 1.5 €/kg to 5.5 €/kg, depending on the year of installation.

The curves also pan to the left, representing the reduction of LCOH in Europe over time. In 2020, 1250 TWh can be generated annually at a cost of less than 5.0 €/kg, while in 2050 all 13,750 TWh available in European seas can be generated at a cost of less than 3.5 €/kg in 2050.

The cheapest hydrogen can be produced at 4.5 €/kg in 2020 and drops to 1.5 €/kg by 2050.

The production cost of gray hydrogen (e.g., from methane cracking) was estimated at 2 in 2020, making W2H projects competitive by 2050. These costs have exploded recently due to the high price of natural gas and are now around 6 €/kg. They could also increase due to a higher carbon tax, making W2H projects even more competitive or bringing them forward.

6.1.2.1. Sensitivity analysis. Since the hypothesis of wind turbine and electrolyzer costs is crucial for the economic evaluation, a sensitivity analysis was performed considering the following variants:

- Wind turbine costs, especially for floating turbines, are difficult to predict. Based on the values predicted by RTE [59], uncertainty margins of ± 400 €/kW in 2030 and ± 600 €/kW in 2050 are considered
- The evolution of the cost of electrolyzers is very uncertain [104]. Alternative higher and lower electrolyzer costs are considered by reducing the β coefficient, which represents the learning curve effect over the years, from −100 to −50 for the higher case and to −150 for the lower case. Thus, an electrolyzer of 100 MW will cost 935 €/kW in 2030 and 800 €/kW in 2050 for the higher case (670 €/kW and 470 €/kW for the lower case)

Fig. 9 plots the evolution of the EAR curves as confidence intervals in 2030 and 2050. The minimum hydrogen cost range is 2.25–2.9 €/kg in 2030, with a potential of 1250 TWh/year at less than 2.6–3.3 €/kg.

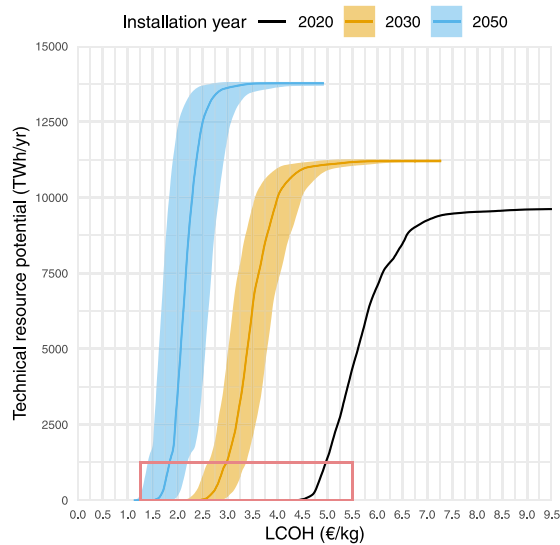


Fig. 9. Evolution of the economic resource with installation years. Shaded area: Resource range sensitized to electrolyzer and wind turbine costs. Rectangle: Focus area of Fig. 10.

In 2050, the cost range drops to 1.2–1.9 €/kg and the potential to 1250 TWh/year at less than 1.3–2.2 €/kg. This variation, which is constant along the EAR curve since it does not depend on depth and distance from the coast, is about ± 0.3 €/kg in 2030 and ± 0.4 €/kg in 2050.

6.1.2.2. Competing usages of offshore wind and pertinence of offshore electrolysis. In the frame of the European Green Deal, installed capacity of offshore wind is expected to increase to 450 GW by 2050 [105]. In a preliminary analysis, we assume that this ocean use will compete with dedicated offshore hydrogen production.

The two facets on Fig. 10 represent the evolution of the low-cost resource (part of the EAR curve highlighted on Fig. 9), depending on whether we assume that the most economical sites identified for onshore electrolysis could be used for W2P. The same diagram shows both the original resource curve that considers W2H and an additional resource curve that represents the economic resource when onshore electrolysis is the only option considered. This analysis highlights the interest in considering offshore electrolysis schemes and leads to the following conclusions:

- When competing uses of offshore wind are taken into account, the LCOH of the cheapest hydrogen increases by about 18% regardless of the year of installation
- Offshore electrolysis has almost no impact on the low-cost resource in 2020, as this solution is not competitive, but significantly reduces LCOH from 2030 onwards, whether or not some areas are reserved for W2P
- Savings from offshore production schemes increase with LCOH, as the most expensive resources are located far from shore and/or in deep waters, where offshore production schemes are most advantageous
- The most economical locations for the 450 GW of W2P do not completely overlap with the best locations for W2H. A resource of about 200 TWh is accessible at a much lower LCOH (-10%) when considering offshore production schemes. In 2050, the cost advantage of W2H schemes can be observed along the entire curve of low-cost resources

6.1.3. By-country potential estimation

The European map of LCOH can also be used for country-level analyzes using exclusive economic zones (EEZs).

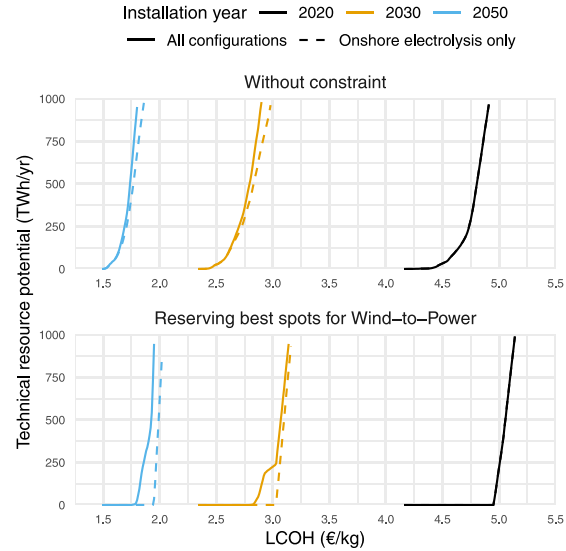


Fig. 10. Evolution of the resource at low LCOH when considering offshore or onshore electrolysis only. Upper plot: All sites are available for hydrogen production; Lower plot: 450 GW of capacity is reserved for W2P.

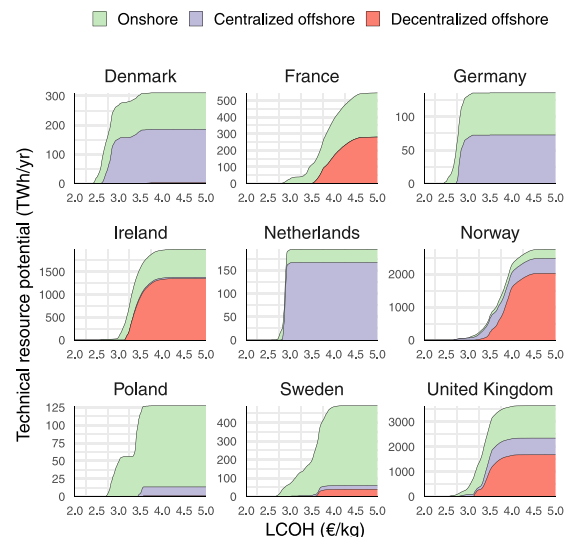


Fig. 11. National EAR curves in 2030, declined by type of connection scheme. Caution: Y axis differs from one country to another.

The EAR curves for nine European countries are presented in Fig. 11, with a particular focus on the most economical connection scheme.

This focus highlights the wide diversity of contexts, as some countries can be identified as suppliers of low-cost hydrogen, such as Denmark, Germany, and the Netherlands, where centralized offshore hydrogen production overtakes the potential but limited total resources are available, while others, such as France, Norway, and Sweden, have large potential but at higher cost. It should be noted that in some countries in the far north, such as Norway, part of the seas are difficult to exploit due to ice cover, so resources here are overestimated. Ireland and the UK both have significant potential with reasonable LCOH, making them important players in future hydrogen production from offshore wind.

These data are of great interest to energy modelers and local stakeholders seeking the best location for W2H projects. For this reason, several datasets are provided for further use and are openly available [106], namely:

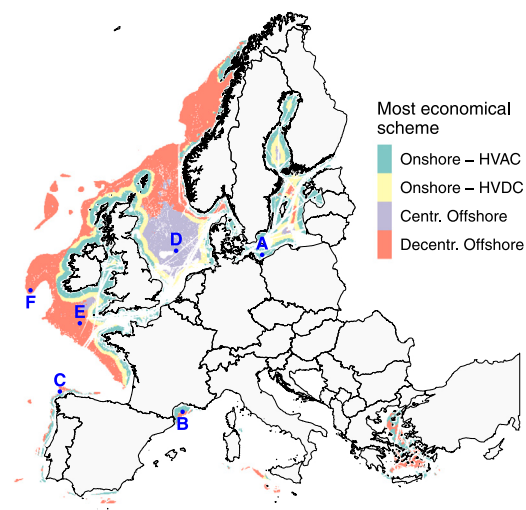


Fig. 12. European map of most economical schemes in 2030. Red points: Study cases for cost comparison (see Section 6.2.1).

Table 23
Characteristics of the sites selected for in-depth cost structure comparison (see the location of points on Fig. 8).

ID	Distance		Depth (m)	lon (°)	lat (°)
	Shore (km)	Port (km)			
A	39.2	205.2	13	14.73	54.36
B	66.0	159.6	126	4.08	42.85
C	45.0	203.8	960	-8.94	43.76
D	248.3	309.2	27	3.51	55.18
E	184.7	253.8	134	-7.83	49.17
F	291.2	437.1	796	-14.30	50.98

- LCOH mapping for each connection scheme, final LCOH, preferred option, and energy production. Where applicable, sensitized cost hypotheses and evolution over the years are included
- The EAR curves at European and national level, including Iceland
- The visualization of the datasets mentioned above

Although Iceland was excluded from the study, its maps and EAR curves are provided as supplementary material.

6.2. Comparison of connection schemes

Fig. 12 depicts the preferred connection scheme for hydrogen production from offshore wind. This map shows that onshore electrolysis is limited to nearshore locations because of the high cost and energy losses due to power cables. HVAC is preferred for nearshore locations. A limited area—mainly in the North Sea—is devoted to centralized offshore electrolysis due to the limited cost of platforms in shallow waters. Finally, decentralized offshore hydrogen generation is the preferred option for far-from-shore and deepwater sites.

6.2.1. Cost structure analysis

Six sites, shown in **Fig. 12**, were selected to cover a variety of typologies in terms of water depth and distance from shore (and port). The characteristics of the selected sites are shown in **Table 23**.

The lifetime costs structure and LCOH for the six sites are shown in **Fig. 13**.

Offshore electrolysis connection schemes offer much lower transmission costs because pipelines are less expensive than power cables. Nevertheless, centralized and decentralized offshore tie-in systems require additional platform and wind turbine adaptation costs, respectively.

Platform costs are high in deep waters for the centralized option, while inter-array costs are non-negligible for the decentralized alternative, as flexible pipes must be laid on the seabed. Ultimately, onshore electrolysis is almost always the most economical option in terms of total lifetime cost, followed by the centralized offshore and decentralized offshore options in that order.

LCOH does not behave exactly like lifetime total cost because of energy losses and wind farm unavailability. Onshore electrolysis is the most economical option for nearshore hydrogen production, although the observed differences in LCOH are smaller than in total cost, and the decentralized offshore scheme is nearly competitive in very deep waters. In contrast, the offshore electrolysis options are by far the more economical when considering far-from-shore locations, with the centralized option preferred for shallow waters and the decentralized option preferred for deep waters. This reversal is due to the low losses in the pipelines and their lower failure rate.

6.2.2. Evolution of break-even points

Due to the evolution of the cost of electrolyzers, the points at which one system is more economical than another change over the years. **Fig. 14** represents the evolution of LCOH offered by each connection scheme with the year of installation. In 2020, the centralized option is preferred almost everywhere except for remote and very deep sites. As seen earlier, the onshore configuration near the coast is still the most economical in 2030, but less competitive than offshore electrolysis. In 2050, offshore connection schemes are preferred in almost all situations except nearshore and in shallow waters.

To emphasize these observations, **Fig. 15** shows the most commonly observed connection schemes, depending on the distance from the coast and depth at the site, based on the evaluation at European scale.

The following observations can be made:

- The break-even point between onshore and offshore hydrogen production in shallow waters (up to 100 m) decreases over time. In 2020, it is more economical to produce hydrogen from electricity transported to shore via power cables than to produce it up to 200 km offshore, while the break-even point is located around 80 km in 2030 and decreases to 50 km by 2050. This is mainly due to the large reduction in electrolyzer costs, which means that the additional cost of installing the electrolyzer offshore is offset by the lower cost of transporting it via pipeline and higher availability.
- The decentralized offshore hydrogen production is preferred to a centralized scheme in deep waters (over 100 m) when the platform costs and inter-array losses become prohibitive. In 2050, the decentralized option is even preferred in shallow waters as the scaling effect of installing small electrolyzers is reduced (see Section 3.1.4.1).
- From 200 m and as the water depth increases, onshore electrolysis becomes more economical than offshore schemes. Indeed, inter-array pipelines are laid on the seabed, while suspended inter-array cables are more economical.
- The break-even point between HVAC and HVDC connections is located around 50 km, which agrees with the literature.

In conclusion, even if offshore electrolysis is more economical, the construction of dedicated wind farms for hydrogen production prevents electricity from being used for other purposes. In fact, the missed opportunity to sell electricity when prices are high and produce hydrogen when they are low could change the balance and expand the relevance of onshore hydrogen production. Nevertheless, offshore electrolysis is by far more economical for far-from-shore sites than its onshore counterpart and should be considered. This analysis is supported by **Fig. 14**, where LCOH differences at nearshore sites are negligible.

Mapping of the preferred option is provided as supplementary material and is openly available [106].

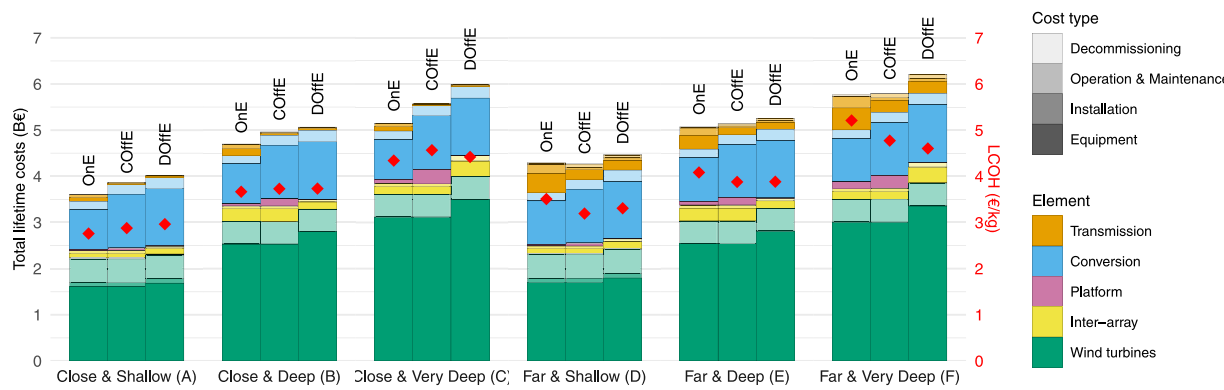


Fig. 13. Lifetime costs structure and LCOH for the six selected sites in 2030 (OnE: Onshore Electrolysis, COFFe: Centralized Offshore Electrolysis, DOffE: Decentralized Offshore Electrolysis).

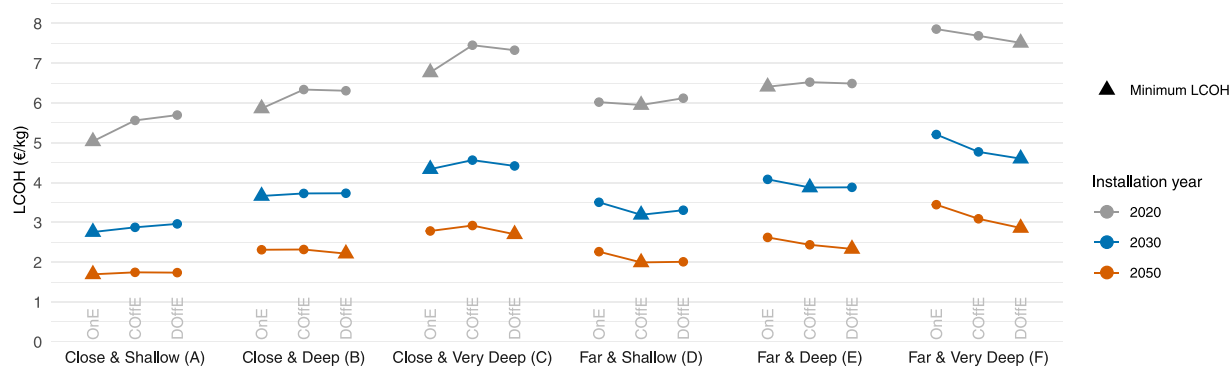


Fig. 14. Evolution of the LCOH with the year of installation (OnE: Onshore Electrolysis, COFFe: Centralized Offshore Electrolysis, DOffE: Decentralized Offshore Electrolysis).

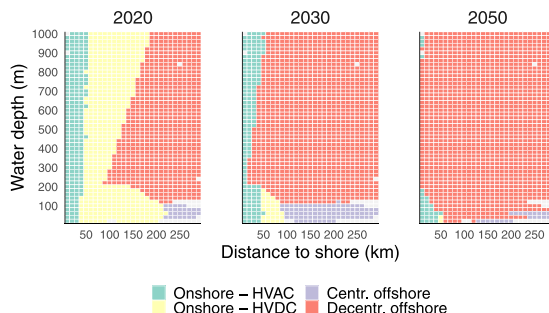


Fig. 15. Most observed connection schemes in European seas depending on the distance to shore and water depth.

7. Conclusions

7.1. Findings and contributions

The first contribution of this work is the development of a detailed bottom-up techno-economic evaluation of offshore W2H projects. This modeling represents a synthesis of specialized models found in both the wind power and hydrogen production literatures.

The second contribution of the work presented in this paper is a resource assessment conducted at European scale using large datasets (wind, bathymetry, port locations) and utilizing the cost modeling mentioned above. This mapping allows the generation of EAR curves sensitized by optimistic and pessimistic cost assumptions for electrolyzers and wind turbines. Variations of the EAR curves that account for future competing W2P developments reveal a 200 TWh potential

where W2H is highly competitive with its power counterpart. Global mapping created with geographic information systems also allows for country-level assessments. Because this data is valuable to decision makers and the energy modeling community, the resulting datasets are open-sourced.

Comparing the economics of the three tie-in systems is the third and final contribution of this work. In particular, it has been shown that offshore production of hydrogen combined with pipeline transport is more economical than onshore electrolysis in many configurations. While offshore production is limited to far-from-shore and deep-water locations in 2020, this option becomes more important over the years: By 2050, onshore electrolysis is more economical only in nearshore and shallow waters.

In summary, this work (1) provided detailed modeling of the costs of offshore wind and hydrogen production at sea, (2) used it for case studies comparing hydrogen production options in different configurations, and (3) conducted a large-scale resource assessment to disseminate to the community.

7.2. Future work

Despite the contributions of this work, some future research should be carried out to deepen the analysis.

First, transportation by tanker could be included in the analysis for very distant and/or very deep sites, which would require proper optimization of hydrogen storage. The hydrogen produced could be transported liquefied or as ammonia.

Second, this analysis does not account for the cost of missed opportunities for electricity generation as dedicated wind farms are considered. Optimizing hydrogen/power generation for onshore electrolysis configurations and considering an additional export cable or fuel cell

for offshore configurations could make the resource even more economical. Similarly, it could be instructive to evaluate hybrid wind-and-solar configurations to further increase electrolyzer utilization rates and reduce the corresponding LCOH.

The adjusted production costs of hydrogen in waters with frequent ice cover, such as in Norway, could also be investigated to identify new opportunities.

Finally, the LCOH was estimated at shore, and the potential cost of connecting to existing infrastructure was not considered. Consequently, LCOH in remote areas such as northern Sweden could be significantly underestimated. On the contrary, existing infrastructure such as decommissioned oil and gas platforms and pipelines could be reused and utilized for hydrogen production. [107–110].

CRediT authorship contribution statement

Antoine Rogeau: Conceptualization, Methodology, Software, Formal analysis, Investigation, Data curation, Writing – original draft, Visualization. **Julien Vieubled:** Conceptualization, Methodology, Writing – review & editing, Supervision. **Matthieu de Coatpont:** Conceptualization, Methodology, Software, Data curation. **Pedro Affonso Nobrega:** Writing – review & editing. **Guillaume Erbs:** Supervision, Project administration. **Robin Girard:** Conceptualization, Methodology, Writing – review & editing, Supervision, Project administration, Funding acquisition.

Declaration of competing interest

The authors declare that they have no known competing financial interests or personal relationships that could have appeared to influence the work reported in this paper.

Data availability

Datasets related to this article can be found at <https://doi.org/10.5281/zenodo.8036703>, an open-source online data repository hosted at Zenodo [106]. The following information is provided:

- Datasets resulting from the modeling are provided in NetCDF format, including maps of LCOH for each connection scheme, final LCOH, energy production, and preferred option.
- The visualization of the above datasets in the form of national maps.
- Dataset of EAR curves at European and national scales, sensitized as in Section 6.1.2.1.
- Visualization of the sensitized EAR curves.

Declaration of Generative AI and AI-assisted technologies in the writing process

During the preparation of this work, the authors used InstaText, GrammarlyGo, and Trinka in order to improve the English quality of the manuscript. After using this tool, the authors reviewed and edited the content as needed and take full responsibility for the content of the publication.

Acknowledgments

This work results from a partnership between Mines Paris - PSL, ENGIE Impact France, and ENGIE SA, in the frame of the program “France Relance/Préservation de l’Emploi R&D” partially funded by the French Ministry of Higher Education and Scientific Research.

Disclaimer

This paper does not reflect the vision of ENGIE Group but only the ideas of the authors.

References

- [1] Mosca L, Palo E, Colozzi M, Iaquaniello G, Salladini A, Taraschi S. Hydrogen in chemical and petrochemical industry. In: Current trends and future developments on (bio-) membranes. Elsevier; 2020, p. 387–410. <http://dx.doi.org/10.1016/B978-0-12-817384-8.00017-0>.
- [2] Kullmann F, Linßen J, Stolten D. The role of hydrogen for the defossilization of the German chemical industry. Int J Hydrogen Energy 2023. <http://dx.doi.org/10.1016/j.ijhydene.2023.04.191>.
- [3] Choi W, Kang S. Greenhouse gas reduction and economic cost of technologies using green hydrogen in the steel industry. J Environ Manag 2023;335:117569. <http://dx.doi.org/10.1016/j.jenvman.2023.117569>.
- [4] Shahabuddin M, Brooks G, Rhamdhani MA. Decarbonisation and hydrogen integration of steel industries: Recent development, challenges and technoeconomic analysis. J Clean Prod 2023;395:136391. <http://dx.doi.org/10.1016/j.jclepro.2023.136391>.
- [5] Marocco P, Gandiglio M, Audisio D, Santarelli M. Assessment of the role of hydrogen to produce high-temperature heat in the steel industry. J Clean Prod 2023;388:135969. <http://dx.doi.org/10.1016/j.jclepro.2023.135969>.
- [6] Fayazi Rad I, Amini M, Ahmadi A, Hoseinzadeh S. Environmental and economic assessments of hydrogen utilization in the transportation sector of Iran. Chem Eng Technol 2023;46(3):435–46. <http://dx.doi.org/10.1002/ceat.202100500>.
- [7] van Renssen S. The hydrogen solution? Nature Clim Change 2020;10(9):799–801. <http://dx.doi.org/10.1038/s41558-020-0891-0>.
- [8] Michael Liebreich/Liebreich Associates. Clean hydrogen ladder, version 4.1. 2021, CC-BY 3.0.
- [9] Balasubramanian R, Abishek A, Gobinath S, Jaivignesh K. Alternative fuel: Hydrogen and its thermodynamic behaviour. J Human Earth Future 2022;3(2):195–203. <http://dx.doi.org/10.28991/HEF-2022-03-02-05>.
- [10] Cihlar J, Villar Lejarreta A, Wang A, Melgar F, Jens J, Rio P. Hydrogen generation in Europe: Overview of costs and key benefits. Technical report, European Commission; 2021, <http://dx.doi.org/10.2833/821682>.
- [11] Wang A, Jens J, Mavins D, Moultag M, Schimmel M, Van der Leun K, et al. Analysing future demand, supply, and transport of hydrogen. Technical report, European Hydrogen Backbone Initiative; 2021.
- [12] Blanco H, Nijs W, Ruf J, Faaij A. Potential for hydrogen and Power-to-Liquid in a low-carbon EU energy system using cost optimization. Appl Energy 2018;232:617–39. <http://dx.doi.org/10.1016/j.apenergy.2018.09.216>.
- [13] IEA. The future of hydrogen - Seizing today's opportunities. Technical report, International Energy Agency; 2019, URL https://www.capenergies.fr/wp-content/uploads/2019/07/the_future_of_hydrogen.pdf.
- [14] Peters R, Vaessen J, Meer Rvd. Offshore hydrogen production in the north sea enables far offshore wind development. OTC; 2020, <http://dx.doi.org/10.4043/30698-MS>.
- [15] Xiang X, Merlin M, Green T. Cost analysis and comparison of HVAC, LFAC and HVDC for offshore wind power connection. In: 12th IET international conference on AC and DC power transmission. ACDC 2016, Institution of Engineering and Technology; 2016, p. 6. <http://dx.doi.org/10.1049/cp.2016.0386>.
- [16] Van Eeckhout B, Van Hertem D, Reza M, Srivastava K, Belmans R. Economic comparison of VSC HVDC and HVAC as transmission system for a 300 MW offshore wind farm. Eur Trans Electr Power 2009. <http://dx.doi.org/10.1002/etep.359>.
- [17] Lazaridis LP. Economic comparison of HVAC and HVDC solutions for large offshore wind farms under special consideration of reliability [Ph.D. thesis], Stockholm: Royal Institute of Technology; 2005, URL <https://www.diva-portal.org/smash/get/diva2:609080/FULLTEXT01.pdf>.
- [18] Lauria S, Schembra M, Palone F, Maccioni M. Very long distance connection of gigawatt-size offshore wind farms: extra high-voltage AC versus high-voltage DC cost comparison. IET Renew Power Gener 2016;10(5):713–20. <http://dx.doi.org/10.1049/iet-rpg.2015.0348>.
- [19] Jiang Z. Installation of offshore wind turbines: A technical review. Renew Sustain Energy Rev 2021;139:110576. <http://dx.doi.org/10.1016/j.rser.2020.110576>.
- [20] Kaiser MJ, Snyder BF. Modeling offshore wind installation costs on the U.S. outer continental shelf. Renew Energy 2013;50:676–91. <http://dx.doi.org/10.1016/j.renene.2012.07.042>.
- [21] Ahn D, Shin S-c, Kim S-y, Kharoufi H, Kim H-c. Comparative evaluation of different offshore wind turbine installation vessels for Korean west-south wind farm. Int J Nav Archit Ocean Eng 2017;9(1):45–54. <http://dx.doi.org/10.1016/j.jinaoe.2016.07.004>.
- [22] Chitteth Ramachandran R, Desmond C, Judge F, Serraris J-J, Murphy J. Floating offshore wind turbines: installation, operation, maintenance and decommissioning challenges and opportunities. 2021, Wind Energy Science Discussions.
- [23] McMorland J, Collu M, McMillan D, Carroll J. Operation and maintenance for floating wind turbines: A review. Renew Sustain Energy Rev 2022;163:112499. <http://dx.doi.org/10.1016/j.rser.2022.112499>.

- [24] Ren Z, Verma AS, Li Y, Teuwen JJ, Jiang Z. Offshore wind turbine operations and maintenance: A state-of-the-art review. *Renew Sustain Energy Rev* 2021;144:110886. <http://dx.doi.org/10.1016/j.rser.2021.110886>.
- [25] Milne C, Jalili S, Maher A. Decommissioning cost modelling for offshore wind farms: A bottom-up approach. *Sustain Energy Technol Assess* 2021;48:101628. <http://dx.doi.org/10.1016/j.seta.2021.101628>.
- [26] Kaiser MJ, Snyder B. Modeling the decommissioning cost of offshore wind development on the U.S. outer continental shelf. *Mar Policy* 2012;36(1):153–64. <http://dx.doi.org/10.1016/j.marpol.2011.04.008>.
- [27] Altuzarra J, Herrera A, Matías O, Urbano J, Romero C, Wang S, et al. Mooring system transport and installation logistics for a floating offshore wind farm in Lannion, France. *J Mar Sci Eng* 2022;10(10):1354. <http://dx.doi.org/10.3390/jmse10101354>.
- [28] Saeed K, McMorland J, Collu M, Coraddu A, Carroll J, McMillan D. Adaptations of offshore wind operation and maintenance models for floating wind. *J Phys Conf Ser* 2022;2362(1):012036. <http://dx.doi.org/10.1088/1742-6596/2362/1/012036>.
- [29] Castro-Santos I, Filgueira-Vizoso A, Lamas-Galdo I, Carral-Couce L. Methodology to calculate the installation costs of offshore wind farms located in deep waters. *J Clean Prod* 2018;170:1124–35. <http://dx.doi.org/10.1016/j.jclepro.2017.09.219>.
- [30] Maienza C, Avossa AM, Ricciardelli F, Scherillo F, Georgakis CT. A comparative analysis of construction costs of onshore and shallow- and deep-water offshore wind Farms. 2019, p. 440–53. http://dx.doi.org/10.1007/978-3-030-12815-9_35.
- [31] Elsner P. Continental-scale assessment of the African offshore wind energy potential: Spatial analysis of an under-appreciated renewable energy resource. *Renew Sustain Energy Rev* 2019;104:394–407. <http://dx.doi.org/10.1016/j.rser.2019.01.034>.
- [32] Patel RP, Nagababu G, Kachhwaha SS, Surisetty VAK. A revised offshore wind resource assessment and site selection along the Indian coast using ERA5 near-hub-height wind products. *Ocean Eng* 2022;254:111341. <http://dx.doi.org/10.1016/j.oceaneng.2022.111341>.
- [33] Arenas-López JP, Badaoui M. Analysis of the offshore wind resource and its economic assessment in two zones of Mexico. *Sustain Energy Technol Assess* 2022;52:101997. <http://dx.doi.org/10.1016/j.seta.2022.101997>.
- [34] Martinez A, Iglesias G. Mapping of the levelised cost of energy for floating offshore wind in the European Atlantic. *Renew Sustain Energy Rev* 2022;154:111889. <http://dx.doi.org/10.1016/j.rser.2021.111889>.
- [35] Martinez A, Iglesias G. Multi-parameter analysis and mapping of the levelised cost of energy from floating offshore wind in the Mediterranean Sea. *Energy Convers Manage* 2021;243:114416. <http://dx.doi.org/10.1016/j.enconman.2021.114416>.
- [36] Beiter P, Musial W, Kilcher L, Maness M, Smith A. An assessment of the economic potential of offshore wind in the united states from 2015 to 2030. Technical report, Golden, CO (United States): National Renewable Energy Laboratory (NREL); 2017, <http://dx.doi.org/10.2172/1349721>.
- [37] Díaz H, Guedes Soares C. An integrated GIS approach for site selection of floating offshore wind farms in the Atlantic continental European coastline. *Renew Sustain Energy Rev* 2020;134:110328. <http://dx.doi.org/10.1016/j.rser.2020.110328>.
- [38] Tercan E, Tapkin S, Latinopoulos D, Dereli MA, Tsiropoulos A, Ak MF. A GIS-based multi-criteria model for offshore wind energy power plants site selection in both sides of the Aegean Sea. *Environ Monit Assess* 2020;192(10):652. <http://dx.doi.org/10.1007/s10661-020-08603-9>.
- [39] Dupré la Tour M-A. Photovoltaic and wind energy potential in Europe – A systematic review. *Renew Sustain Energy Rev* 2023;179:113189. <http://dx.doi.org/10.1016/j.rser.2023.113189>.
- [40] Caglayan DG, Ryberg DS, Heinrichs H, Linßen J, Stolten D, Robinius M. The techno-economic potential of offshore wind energy with optimized future turbine designs in Europe. *Appl Energy* 2019;255:113794. <http://dx.doi.org/10.1016/j.apenergy.2019.113794>.
- [41] Hundley G, Freeman K. Unleashing Europe's offshore wind potential: A new resource assessment. Technical report, Wind Europe; 2017.
- [42] Guedes Soares C, Bento AR, Gonçalves M, Silva D, Martinho P. Numerical evaluation of the wave energy resource along the Atlantic European coast. *Comput Geosci* 2014;71:37–49. <http://dx.doi.org/10.1016/j.cageo.2014.03.008>.
- [43] Calado G, Castro R. Hydrogen production from offshore wind parks: Current situation and future perspectives. *Appl Sci* 2021;11(12):5561. <http://dx.doi.org/10.3390/app11125561>.
- [44] Ibrahim OS, Singlitico A, Proskovics R, McDonagh S, Desmond C, Murphy JD. Dedicated large-scale floating offshore wind to hydrogen: Assessing design variables in proposed typologies. *Renew Sustain Energy Rev* 2022;160:112310. <http://dx.doi.org/10.1016/j.rser.2022.112310>.
- [45] Luo Z, Wang X, Wen H, Pei A. Hydrogen production from offshore wind power in South China. *Int J Hydrogen Energy* 2022;47(58):24558–68. <http://dx.doi.org/10.1016/j.ijhydene.2022.03.162>.
- [46] Singlitico A, Østergaard J, Chatzivasileiadis S. Onshore, offshore or in-turbine electrolysis? Techno-economic overview of alternative integration designs for green hydrogen production into offshore wind power hubs. *Renew Sustain Energy Trans* 2021;1:100005. <http://dx.doi.org/10.1016/j.rset.2021.100005>.
- [47] Lüth A, Seifert PE, Egging-Bratseth R, Weibezahn J. How to connect energy islands: Trade-offs between hydrogen and electricity infrastructure. *Appl Energy* 2023;341:121045. <http://dx.doi.org/10.1016/j.apenergy.2023.121045>.
- [48] Lucas TR, Ferreira AF, Santos Pereira R, Alves M. Hydrogen production from the WindFloat Atlantic offshore wind farm: A techno-economic analysis. *Appl Energy* 2022;310:118481. <http://dx.doi.org/10.1016/j.apenergy.2021.118481>.
- [49] Giampieri A, Ling-Chin J, Roskilly AP. Techno-economic assessment of offshore wind-to-hydrogen scenarios: A UK case study. *Int J Hydrogen Energy* 2023. <http://dx.doi.org/10.1016/j.ijhydene.2023.01.346>.
- [50] Kim A, Kim H, Choe C, Lim H. Feasibility of offshore wind turbines for linkage with onshore green hydrogen demands: A comparative economic analysis. *Energy Convers Manage* 2023;277:116662. <http://dx.doi.org/10.1016/j.enconman.2023.116662>.
- [51] Jiang Y, Huang W, Yang G. Electrolysis plant size optimization and benefit analysis of a far offshore wind-hydrogen system based on information gap decision theory and chance constraints programming. *Int J Hydrogen Energy* 2022;47(9):5720–32. <http://dx.doi.org/10.1016/j.ijhydene.2021.11.211>.
- [52] Miao B, Giordano L, Chan SH. Long-distance renewable hydrogen transmission via cables and pipelines. *Int J Hydrogen Energy* 2021;46(36):18699–718. <http://dx.doi.org/10.1016/j.ijhydene.2021.03.067>.
- [53] d'Amore Domenech R, Leo TJ, Pollet BG. Bulk power transmission at sea: Life cycle cost comparison of electricity and hydrogen as energy vectors. *Appl Energy* 2021;288:116625. <http://dx.doi.org/10.1016/j.apenergy.2021.116625>.
- [54] Komorowska A, Benalcazar P, Kamiński J. Evaluating the competitiveness and uncertainty of offshore wind-to-hydrogen production: A case study of Poland. *Int J Hydrogen Energy* 2023;48(39):14577–90. <http://dx.doi.org/10.1016/j.ijhydene.2023.01.015>.
- [55] Dinh QV, Dinh VN, Mosadeghi H, Todesco Pereira PH, Leahy PG. A geospatial method for estimating the levelised cost of hydrogen production from offshore wind. *Int J Hydrogen Energy* 2023;48(40):15000–13. <http://dx.doi.org/10.1016/j.ijhydene.2023.01.016>.
- [56] Serna A, Tadeo F. Offshore hydrogen production from wave energy. *Int J Hydrogen Energy* 2014;39(3):1549–57. <http://dx.doi.org/10.1016/j.ijhydene.2013.04.113>.
- [57] Babarit A, Gorintin F, de Belizal P, Neau A, Bordogna G, Gilloteaux J-C. Exploitation of the far-offshore wind energy resource by fleets of energy ships – Part 2: Updated ship design and cost of energy estimate. *Wind Energy Sci* 2021;6(5):1191–204. <http://dx.doi.org/10.5194/wes-6-1191-2021>.
- [58] Bosch J, Staffell I, Hawkes AD. Global levelised cost of electricity from offshore wind. *Energy* 2019;189:116357. <http://dx.doi.org/10.1016/j.energy.2019.116357>.
- [59] RTE. 11 - L'analyse économique. In: *Futurs énergétiques 2050*. Réseau de Transport d'Électricité; 2021, p. 533–645, URL https://assets.rte-france.com/prod/public/2022-06/FE2050%20_Rapport%20complet_11.pdf.
- [60] Danish Energy Agency. Technology data for energy carrier generation and conversion. 2017, URL <https://ens.dk/en/our-services/projections-and-models/technology-data/technology-data-renewable-fuels>.
- [61] BVG Associates. Guide to an offshore wind farm. Technical report, Catapult: The Crown Estate; 2019, URL <https://www.thecrownestate.co.uk/media/2861/guide-to-offshore-wind-farm-2019.pdf>.
- [62] Timmers V, Egea-Álvarez A, Li R, Xu L. All-DC offshore wind farms: When are they more cost-effective than AC designs? *IET Renew Power Gener* 2022. <http://dx.doi.org/10.1049/rpg2.12550>.
- [63] National Grid ESO. Electricity ten years statement - Appendix E technology. Technical report, NationalGridESO; 2013, URL <https://www.nationalgrideso.com/document/46916/download>.
- [64] Breunis W. *Hydrogen gas production from offshore wind energy: A cost-benefit analysis of optionality through grid connection* [Ph.D. thesis], Delft University of Technology; 2021.
- [65] d'Amore Domenech R, Leo TJ. Sustainable hydrogen production from offshore marine renewable farms: Techno-energetic insight on seawater electrolysis technologies. *ACS Sustain Chem Eng* 2019;7(9):8006–22. <http://dx.doi.org/10.1021/acssuschemeng.8b06779>.
- [66] Reksten AH, Thomassen MS, Möller-Holst S, Sundseth K. Projecting the future cost of PEM and alkaline water electrolyzers; a CAPEX model including electrolyser plant size and technology development. *Int J Hydrogen Energy* 2022;47(90):38106–13. <http://dx.doi.org/10.1016/j.ijhydene.2022.08.306>.
- [67] Newborough M, Cooley G. Green hydrogen: water use implications and opportunities. *Fuel Cells Bull* 2021;2021(12):12–5. [http://dx.doi.org/10.1016/S1464-2859\(21\)000658-1](http://dx.doi.org/10.1016/S1464-2859(21)000658-1).
- [68] Kim J, Park K, Yang DR, Hong S. A comprehensive review of energy consumption of seawater reverse osmosis desalination plants. *Appl Energy* 2019;254:113652. <http://dx.doi.org/10.1016/j.apenergy.2019.113652>.
- [69] Lerch M, De-Prada-Gil M, Molins C. A metaheuristic optimization model for the inter-array layout planning of floating offshore wind farms. *Int J Electr Power Energy Syst* 2021;131:107128. <http://dx.doi.org/10.1016/j.ijepes.2021.107128>.
- [70] Collin A, Nambiar A, Bould D, Whitby B, Moonem M, Schenkman B, et al. Electrical components for marine renewable energy arrays: A techno-economic review. *Energies* 2017;10(12):1973. <http://dx.doi.org/10.3390/en10121973>.

- [71] Djapic P, Strbac G. Cost benefit methodology for optimal design of offshore transmission systems. Technical report, Centre for Sustainable Electricity and Distributed Generation; 2008, URL <https://docplayer.net/19438524-Cost-benefit-methodology-for-optimal-design-of-offshore-transmission-systems.html>.
- [72] Domínguez-García JL, Rogers DJ, Ugalde-Loo CE, Liang J, Gomis-Bellmunt O. Effect of non-standard operating frequencies on the economic cost of offshore AC networks. *Renew Energy* 2012;44:267–80. <http://dx.doi.org/10.1016/j.renene.2012.01.093>.
- [73] Ikhennicheu M, Lynch M, Doole S, Borsiade F, Wendt F, Schwarzkopf M-A, et al. D3.1 Review of the state of the art of dynamic cable system design. Technical report, INNOSEA; 2020, URL <https://corewind.eu/wp-content/uploads/files/publications/COREWIND-D3.1-Review-of-the-state-of-the-art-of-dynamic-cable-system-design.pdf>.
- [74] Rapha JI, Domínguez JL. Suspended cable model for layout optimisation purposes in floating offshore wind farms. *J Phys Conf Ser* 2021;2018(1):012033. <http://dx.doi.org/10.1088/1742-6596/2018/1/012033>.
- [75] Weerheim R. Development of dynamic power cables for commercial floating wind farms. Technical report, TU Delft; 2018, URL <http://resolver.tudelft.nl/uuid:487ba1e5-2764-4e96-808c-a9ee2772219d>.
- [76] Bai Y, Bai Q. Subsea cost estimation. In: Subsea Engineering Handbook. Elsevier; 2010, p. 159–92. <http://dx.doi.org/10.1016/B978-1-85617-689-7.10006-8>.
- [77] Tranberg B, Kratmann KK, Stege J. Determining offshore wind installation times using machine learning and open data. 2019.
- [78] Castro Santos L, Ferreño González S, Diaz Casas V. Methodology to calculate mooring and anchoring costs of floating offshore wind devices. *Renew Energy Power Qual J* 2013;268–72. <http://dx.doi.org/10.24084/repqj11.276>.
- [79] Jalili S, Maher A, Ivanovic A. Cost modelling for offshore wind farm decommissioning - Decomtools 2022. Technical report, 2022, URL https://northsearegion.eu/media/19936/cost-modelling_final_2022.pdf.
- [80] Herdiyanti J. Comparisons study of S-Lay and J-Lay methods for pipeline installation in ultra deep water [Ph.D. thesis], University of Stavanger; 2013, URL <https://core.ac.uk/download/pdf/30921158.pdf>.
- [81] Rahmat M. Y. Pipe-laying method in offshore / subsea construction. 2022, URL <https://indonesiare.co.id/id/article/pipeline-laying-method-in-offshore-subsea-construction>.
- [82] Europacable. An introduction to high voltage direct current (HVDC) subsea cables systems. Technical report, Europacable; 2012, URL <https://europacable.eu/wp-content/uploads/2021/01/Introduction-to-HVDC-Subsea-Cables-16-July-2012.pdf>.
- [83] Stehly T, Beiter P, Duffy P. 2019 cost of wind energy Review. Technical report, Golden, CO: National Renewable Energy Laboratory; 2020, URL <https://www.nrel.gov/docs/fy21osti/78471.pdf>.
- [84] Dewan A, Asgarpour M. Reference O&M concepts for near and far offshore wind Farms. Technical report, ECN; 2016, URL <https://publicaties.ecn.nl/PdfFetch.aspx?nr=ECN-E--16-055>.
- [85] Turc Castellà X. Operation and maintenance costs for offshore wind farm - Analysis and strategies to reduce O&M costs [Ph.D. thesis], Universitat Politècnica de Catalunya; 2020, URL <https://upcommons.upc.edu/bitstream/handle/2117/329731/master-thesis-xavier-turc-castell-.pdf>.
- [86] V. Taboada J, Diaz-Casas V, Yu X. Reliability and maintenance management on OffShore wind turbines (OWTs). *Energies* 2021;14(22):7662. <http://dx.doi.org/10.3390/en14227662>.
- [87] Cevasco D, Koukoura S, Kolios A. Reliability, availability, maintainability data review for the identification of trends in offshore wind energy applications. *Renew Sustain Energy Rev* 2021;136:110414. <http://dx.doi.org/10.1016/j.rser.2020.110414>.
- [88] Harman K, Walker R, Wilkinson M. Availability trends observed at operational wind farms. In: European wind energy conference 2008. 2008.
- [89] Avanessova N, Gray A, Lazakis I, Thomson RC, Rinaldi G. Analysing the effectiveness of different offshore maintenance base options for floating wind farms. *Wind Energy Sci* 2022;7(2):887–901. <http://dx.doi.org/10.5194/wes-7-887-2022>.
- [90] Cai Y, Bréon F-M. Wind power potential and intermittency issues in the context of climate change. *Energy Convers Manage* 2021;240:114276. <http://dx.doi.org/10.1016/j.enconman.2021.114276>.
- [91] Brosschot S. Comparing hydrogen networks and electricity grids for transporting offshore wind energy to shore in the North Sea region. A spatial network optimisation approach [Ph.D. thesis], Utrecht University; 2022, URL <https://studenttheses.uu.nl/handle/20.500.12932/43157?show=full>.
- [92] Lepikhin A, Leschenko V, Makhotov N. Defects assessment in subsea pipelines by risk criteria. In: Issues on risk analysis for critical infrastructure protection. IntechOpen; 2021, <http://dx.doi.org/10.5772/intechopen.94851>.
- [93] De Stefani V, Carr P. A model to estimate the failure rates of offshore pipelines. In: 2010 8th international pipeline conference, vol. 4. ASMEDC; 2010, p. 437–47. <http://dx.doi.org/10.1115/IPC2010-31230>.
- [94] EMODnet. Human activities. 2022, URL <https://emodnet.ec.europa.eu/en/human-activities>.
- [95] European Commission – Eurostat/GISCO. NUTS dataset. 2021, URL <https://ec.europa.eu/eurostat/web/gisco/geodata/reference-data/administrative-units-statistical-units/nuts>.
- [96] EMODnet. Bathymetry. 2018, URL <https://emodnet.ec.europa.eu/en/bathymetry>.
- [97] Global Fishing Watch. Datasets and code: Apparent fishing effort. 2019, URL <https://globalfishingwatch.org/dataset-and-code-fishing-effort>.
- [98] Hersbach H, Bell B, Berrisford P, Biavati G, Horányi A, Muñoz Sabater J, et al. ERA5 hourly data on single levels from 1940 to present. In: Copernicus climate change service (C3S) climate data store (CDS). 2023, <http://dx.doi.org/10.24381/cds.adbb2d47>.
- [99] UNEP-WCMC, IUCN. Protected planet: The world database on protected areas (WDPA). 2023, URL <https://www.protectedplanet.net/en/thematic-areas/wdpa?tab=WDPA>.
- [100] Maritime Safety Office. World port index. 2019, URL <https://msi.nga.mil/Publications/WPI>.
- [101] Gualtieri G. Reliability of ERA5 reanalysis data for wind resource assessment: A comparison against tall towers. *Energies* 2021;14(14):4169. <http://dx.doi.org/10.3390/en14144169>.
- [102] Borrmann R, Rehfeldt K, Wallash A-K, Lüers S. Capacity densities of European offshore wind farms. Technical report, Deutsche Windguard; 2018, URL https://vasab.org/wp-content/uploads/2018/06/BalticLINes_CapacityDensityStudy_June2018-1.pdf.
- [103] Bulder B, Bot E, Bedon G. Optimal wind farm power density analysis for future offshore wind farms. ECN; 2018, URL <https://www.humsterlandenergie.nl/resources/LInks-duurzaam/Linkpagina/Optimal-wind-farm-power-density-analysis-for-future-offshore-wind-farms.pdf>.
- [104] IRENA. Green hydrogen cost reduction: Scaling up electrolyzers to meet the 1.5°C climate goal. Technical report, Abu Dhabi: International Renewable Energy Agency; 2020, URL <https://www.irena.org/publications/2020/Dec/Green-hydrogen-cost-reduction>.
- [105] European Commission. A clean planet for all. 2018.
- [106] Rogeau A, Girard R, De Coaptont M, Vieubled J, Erbs G, Affonso Nobrega P. Techno-economic evaluation and resource assessment of hydrogen production through offshore wind farms: A European perspective - Supplementary material. Zenodo; 2023, <http://dx.doi.org/10.5281/zenodo.8036703>.
- [107] Donkers K. Hydrogen production on offshore platforms - A techno-economic analysis [Ph.D. thesis], Utrecht University; 2020, URL <https://studenttheses.uu.nl/bitstream/handle/20.500.12932/37491/The%20thesis%20Koen%20Donkers%20-20%20Final%20version.pdf?sequence=1>.
- [108] Braga J, Santos T, Shadman M, Silva C, Assis Tavares LF, Estefen S. Converting offshore oil and gas infrastructures into renewable energy generation plants: An economic and technical analysis of the decommissioning delay in the Brazilian case. *Sustainability* 2022;14(21):13783. <http://dx.doi.org/10.3390/su142113783>.
- [109] ACER. Transporting pure hydrogen by repurposing existing gas infrastructure: overview of existing studies and reflections on the conditions for repurposing. Technical report, European Union Agency for the Cooperation of Energy Regulators; 2021, URL https://acer.europa.eu/Official_documents/Acts_of_the_Agency/Publication/Transporting%20Pure%20Hydrogen%20by%20Repurposing%20Existing%20Gas%20Infrastructure_Overview%20of%20Studies.pdf.
- [110] Cauchois G, Renaud-Bezot C, Simon M, Gentile V, Carpenter M, Even Torbergsen L. Re-stream - Study on the reuse of oil and gas infrastructure for hydrogen and CCS in Europe. Technical report, Carbon Limits; 2021, URL https://www.concawe.eu/wp-content/uploads/Re-stream-final-report_Oct2021.pdf.